THE UNIVERSITY OF MANITOBA

A DYNAMIC NUCLEAR MAGNETIC RESONANCE STUDY OF FLUORINE EXCHANGE IN TETRAPROPYLAMMONIUM METHYLTETRAFLUOROSILICATE

by

RONALD KIRK MARAT

A THESIS

SUBMITTED TO THE FACULTY OF GRADUATE STUDIES

IN PARTIAL FULFILMENT OF THE REQUIREMENTS FOR THE DEGREE

OF MASTER OF SCIENCE

DEPARTMENT OF CHEMISTRY

WINNIPEG

MANITOBA

APRIL 1976

"A DYNAMIC NUCLEAR MAGNETIC RESONANCE STUDY OF FLUORINE EXCHANGE IN TETRAPROPYLAMMONIUM METHYLTETRAFLUOROSILICATE"

by

RONALD KIRK MARAT

A dissertation submitted to the Faculty of Graduate Studies of the University of Manitoba in partial fulfillment of the requirements of the degree of

MASTER OF SCIENCE

ABSTRACT

A dynamic nuclear magnetic resonance lineshape analysis has been employed in a mechanistic study of the intermolecular fluorine exchange found in the methyltetrafluorosilicate moiety. The exchange is found to be second order in methanol and -0.2 to -0.5 order in the parent fluorosilicate salt. These results are shown to be inconsistent with the previously described mechanisms, and alternate mechanisms based on expansion of the coordination around silicon from five to six are presented. The exchange is found to be inhibited by Lewis-bases such as pyridine. The apparent exchange rate is sensitive to the fluorine spin-lattice relaxation time, under certain circumstances.

ACKNOWLEDGEMENTS

I would like to thank Dr. A. F. Janzen for his continual patience and guidance; the loan of his typewriter is also greatly appreciated.

Thanks are also due to Mr. Wayne Buchanon for running the mass spectra, Dr. Leonard Kruczynski for help with the computer program and to Dr. T. Schaefer for his help with the NMR spectroscopy and the use of the HA 100 spectrometer.

The financial support of the University of Manitoba is greatfully acknowledged.

Finally, special thanks are due to Diana Dueck, whose understanding and patience are source of inspiration. Her help in the proof-reading and typing of this thesis are also appreciated.

CONTENTS

LIST OF TABLES

LIST OF FIGURES

VITA

NAME Ronald Kirk Marat

BORN Winnipeg, Manitoba, 1952.

EDUCATED

PRIMARY Ray M. Schmidt School
Garden Grove, California, USA

Prendergast School
Winnipeg, Manitoba

SECONDARY Windsor Park Collegiate
Winnipeg Manitoba

UNIVERSITY University of Manitoba
Winnipeg, Manitoba
B.Sc. (Hons) 1974
M.Sc. 1976

PUBLICATIONS "Reaction of Xenon Difluoride, Part II. Oxidative Fluorination of Phosphorus and Iodine Compounds and Cleavage of Silicon-Sulfur and Silicon-Nitrogen Bonds." J. A. Gibson, R. K. Marat and A. F. Janzen, Can. J. Chem., 53, 3044 (1975).

"Electron-Coupled Through-Space or Fragment Spin-Spin Coupling Between ^{19}F Nuclei." T. Schaefer, W. Niemczura and K. Marat, J.

Chem. Soc. Faraday II, 71, 1526 (1975).

"The Sign of the 'Through-Space' Spin-Spin Coupling Between Methyl Protons and The Fluorine Nucleus in 2,6-Dimethylbenzoyl Fluoride." T. Schaefer, K. Chum, K. Marat and R. E. Wasylishen, Accepted for Publication, Can. J. Chem.

"Synthesis of Phosphorus and Silicon Fluorides and Mechanisms of Ligand Exchange." R. K. Marat and A. F. Janzen, presented at the 58th Canadian Chemical Conference, May, 1975.

"Nuclear Magnetic Resonance and Molecular Orbital Studies of the Fluoromethyl Group in some Benzylfluoride Derivatives." T. Schaefer, J. B. Rowbotham, W. J. E. Parr, K. Marat and A. F. Janzen, Accepted for Publication, Can. J. Chem.

CHAPTER 1 NATURE OF THE PROBLEM

This study represents part of the continuing interest in this laboratory in the exchange mechanisms of the main group fluorides.[2-6] In particular, the work described in this thesis is a dynamic nuclear magnetic resonance (dnmr) study of the intermolecular fluorine exchange process in the five coordinate silicate salt tetrapropylammonium methyltetrafluorosilicate, $[CH_3SiF_4^-][N(C_3H_7)_4]$.† This salt was first prepared by Klanberg and Muetterties [1] in 1968, who found that the $CH_3SiF_4^-$ ion underwent two distinct types of exchange processes: an intramolecular rearrangement of the fluorines which results in the four fluorines being magnetically and chemically equivalent, and an intermolecular exchange which proceeds at a rate fast enough to cause the loss of nuclear spin-spin coupling between the fluorines and the protons in the methyl group. The structure of the ion was assumed to be trigonal bipyramidal with the methyl group occupying one of the equatorial sites, analagous to the structure of $(C_6H_5)_2SiF_3^-$.[1] The intramolecular rearrangement of a trigonal bipyramid has been recently reviewed, and will not be of great concern to this study.[7]

---

† For brevity, tetrapropylammonium methyltetrafluorosilicate will often be referred to by the formula of the anion, viz $CH_3SiF_4^-$.

The intermolecular exchange, however, has been the subject of much speculation, but no kinetic studies have been carried out. The mechanisms proposed by the original authors were:

1. A bimolecular exchange involving fluorine bridged dimers.

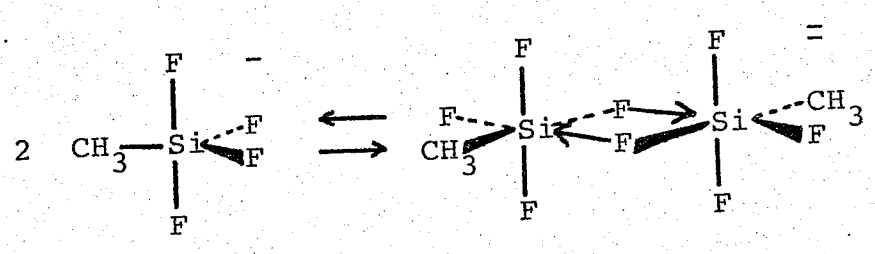

2. A dissociative or ionization prosess.

$$CH_3SiF_4^- \rightleftharpoons CH_3SiF_3 + F^-$$

The basis that they used for postulating these mechanisms was simple analogy to processes known or assumed to occur among the other main group inorganic fluorides (see section 2.1 and references therein for examples of these other mechanisms). For the $CH_3SiF_4^-$ ion they favoured the dissociative mechanism, while for some of the other members of this series, notably SiF_5^-, the first mechanism was favoured.

Workers in this laboratory have found that other mechanisms might be the predominant mechanism of inter-

molecular fluorine exchange. Gibson,[2,3] in a study of the acceptor properties of the SiF_5^- ion, found that the exchange was caused by the presence of trace quantities of moisture. The addition of a drying agent (hexamethyldisilazane) reduced the rate of fluorine exchange, on a nuclear magnetic resonance time scale, to almost zero. Similar effects were noted for $CH_3SiF_4^-$, suggesting that a common mechanism was the cause of exchange in both ions. Many similar cases of catalysis by impurities exist among the other main group inorganic fluorides (section 2.2 and references therein).

In order to help clarify the mechanism of fluorine exchange in these salts, it was decided to undertake a thorough kinetic study of the exchange process in the $CH_3SiF_4^-$ ion, this ion being particularly suitable for dnmr studies because of the nuclear spin-spin coupling between the fluorines and the methyl group.

To accomplish this it was necessary to generate proton magnetic resonance line shapes for a group of three equivalent protons coupled to a group of four equivalent fluorines undergoing intermolecular exchange. Since no examples of a similar system were available in the literature, and none of the generally available line-shape programs appeared capable of solving this problem, it was necessary to derive suitable expressions for the

simulation of the spectra. The McConnell [14] formulation on the Bloch [10] equations was chosen as being the most suitable for this study. The procedure employed was similar to that of Reeves and Shaw,[15] except that matrix manipulation yielded an analytical expression that could be used with the quantum mechanical lineshape programs available to the author. This method of describing the lineshape phenomenon has the advantage of being intuitively understood by someone not versed in the fine points of quantum statistics (such is the case with the author).

Methanol was chosen as the exchange catalyst because it is completely soluble in methylene chloride and the quantities required for exchange were easily measured by standard techniques.

CHAPTER 2 INTRODUCTION

2.1 The dynamic nuclear magnetic resonance technique

Nuclear magnetic resonance spectroscopy provides a convenient method for the study of rate processes that have rates of 10^{-1} to 10^{5} s^{-1}. Consider a situation in which the members of an ensemble of nuclei can exist with equal probability in one of two magnetic environments, A or B, with a difference in Larmor (resonance) frequency of δ_{AB}. If the lifetime in each site is long compared to T_2, the transverse relaxation time, the spectrum will consist of two lines at the resonance frequencies of A and B with line widths ($\Delta\nu_{\frac{1}{2}}$) characteristic of the relaxation time of the nuclei in that situation.

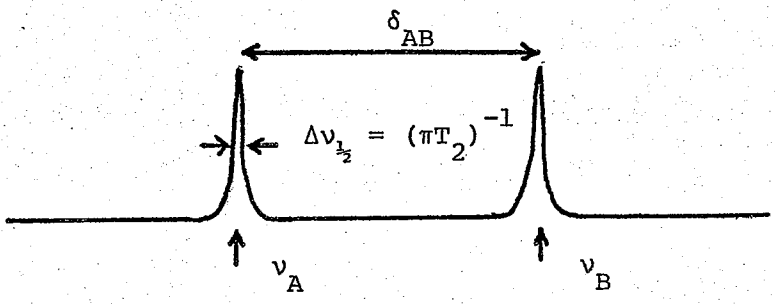

Now, if some mechanism can transfer some of the A type nuclei into site B at the same time that the B's are being transfered into A, a change in the lineshape will occur, the magnitude of which depends on the rate at which this exchange of sites can take place. As the exchange rate

approaches T_2^{-1} the lines will broaden due to a shortening of the lifetime in each site. This effect is a consequence of the uncertainty principle, and is known as "lifetime broadening". Since the lifetime in each site is still longer than the inverse of the frequency difference between the sites, δ_{AB}^{-1}, all of the phase coherence aquired by the A nuclei will be lost by the time that the nuclei return to A. At this point the exchange may be thought of as another T_2 process. This results in a line width of:

$$\Delta\nu_{\frac{1}{2}} = \frac{1}{\pi T_2} + \frac{1}{\pi\tau}$$

where τ is the mean lifetime between exchanges. If the exchange rate approaches the frequency difference between the sites, some of the phase coherence will be maintained between exchanges. The nuclei at site A will start to take on some of the characteristics of B and vice versa. At this point the lines become very broad, and a decrease in the peak separation is noticed. The following diagram provides an illustration of this concept.

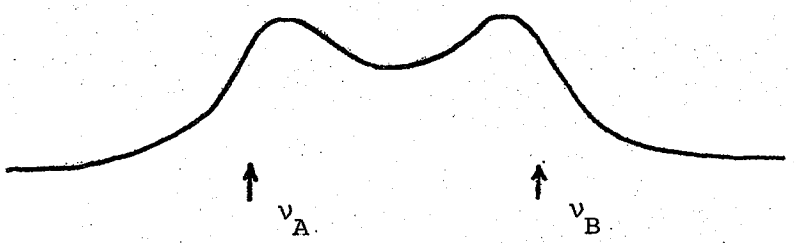

At very high exchange rates all phase coherence will be maintained between exchanges, and furthermore, since the nuclei spend as much time in site A as in site B, a single peak at a frequency that is the average of the two site frequencies is observed. Several approaches have evolved in the attempt to provide a more quantitative description of this effect; a brief outline of these is given below:

a The Bloch-McConnell method

The equations of motion describing the nmr phenomenon were first derived by Bloch.[10] The effects of chemical exchange were first introduced by Gutowsky's group, who employed their modified Bloch equations to study the hindered rotation about the carbonyl-nitrogen bond in dimethylformamide and the related acetamide.[10-13] Piette and Anderson [34] generalized the method to account for multiple sites, with the restriction that the probability of a transfer from site A to site B was proportional to the fractional population of site B. This was applied to a study of bond rotation barriers in alkyl nitrates, and a similar technique was employed by Arnold in a study of proton exchange in ethanol.[35]

A direct introduction of exchange terms into the Bloch equations was proposed by McConnell in 1958.[14] When written in matrix form and solved for the usual steady-state conditions, this method may be generalized to account for

any number of sites with exchange occurring between any or all of the sites.[15,16,21] Many cases of both inter- and intramolecular exchange have been studied by this method,[17-20] and the list of references is by no means exhaustive. Several reviews on the use of the Bloch equations for the study of chemical exchange reactions have also appeared.[21-23,55,56] It must be noted, however, that the Bloch equations are subject to restrictions. At this point, a quotation from a paper by Reeves and Shaw[15] is appropriate: "the use of the modified Bloch equations is restricted to first-order spectra so that the nuclear spin isochromats associated with distinct sites of differing Larmor frequency may be considered to be independent except to chemical exchange effects."

b The density matrix (quantum mechanical) approach

An alternate method for the calculation of exchange broadened nmr spectra has been developed by several groups.[27-34,37] This technique employs a branch of quantum statistics known as "density matrix theory", which is a stochastic matrix representation of Markov probability chain.[57] This theory allows for spin-spin coupling of any magnitude between the sites, and provides for a simplification of the exchange process in terms familiar to chemists, that is: chemical shifts, coupling constants and permutations between nuclei. A detailed description of the

density matrix theory and its applications to nmr spectroscopy, including intramolecular exchange in an "ABX" spin system, has been given by Goodwin.[44]

Many refinements of this theory have been introduced in recent years. Two of these are: the extension of Alexander's work by Whitesides,[37] and the method developed by Jesson and Meakin for separating nmr distinguishable mechanisms by the application of group theory.[38]

The most notable development, however, has been the reformulation of the problem in Liouville space by Binsch and Kleier.[39] With appropriate symmetry and equivalence factoring this technique has enabled computer programs to be written that will handle systems of up to six tightly coupled spins with hundreds of lines.[42,43] These programs are quite simple to use, requiring only chemical shifts, coupling constants, T_2 and a nuclear permutation vector which describes which nuclei become what after the exchange. They can also simulate the spectra in cases where the exchange is non-mutual. In this case the nuclei can exist in more than two configurations and the lifetimes in each situation are not necessarily equal (note that the concept of nuclear situation or configuration is distinct from the concept of "site" used in the Bloch equations). Unfortunately, these programs are of little use for prob-

lems involving intermolecular exchange.

c Pulse methods

All of the methods described thus far have been a description of the spectrum in the frequency domain where the magnetization is plotted as a function of frequency. It is possible though, to study the process in the time domain, since the time interval between repetitive events and the frequency of the events are inversely related.

This approach was developed by Gutowsky's group,[45-52] who have applied the pulse sequence of Carr and Purcell [53] to the loss of transverse magnetization resulting from an exchange process. In the absence of exchange, the amplitude of the spin echoes following each pulse in the Carr-Purcell sequence decay in a purely exponential manner, characterized by a time constant T_2. If an exchange process can transfer magnetization among the various sites, an additional loss of magnetization can occur. The decay resulting from this process is not exponential. Both the Bloch [10,45] and the density matrix[47,50] methods have been employed in the mathematical analysis of this effect. The analysis gives values for the site frequencies, T_2, the site populations and the pre-exchange lifetime.

Advantages of the pulse methods include: separability of the various spectral parameters, making iterative fits to all parameters possible; and a greater dynamic range of

rates.

The reasons that the technique has not become more popular are: the high computational requirements, some unresolved conflicts concerning the validity of the results obtained, and a general unfamiliarity with the methods of pulsed nmr spectroscopy. The increasing popularity of pulse spectrometers may change this situation, though, due to the availability of suitable apparatus and a larger number of people trained in the use of pulse nmr techniques.

An excellent book reviewing all aspects of dynamic nuclear magnetic resonance spectroscopy has recently (1975) appeared.[55] This work is edited by L. M. Jackman and F. A. Cotton, and contains articles by many of the leading people in the field of magnetic resonance.

2.2 Exchange processes in main group inorganic fluorides

It is instructive at this point to review some of the exchange reactions found to occur within the nmr time scale among the group III to group VII and Noble gas fluorides. The examples given are a representative sampling intended to show a few of the sundry mechanisms that have been postulated, and some of the difficulties encountered. Particular emphasis has been placed on the possibility of catalysis by impurities as one of the mechanisms for exchange.

Boron trifluoride has been found to undergo a bimolecular exchange in the presence of Bu_4NPF_6 (Bu= n-C_4H_9).[58] The reaction was found to be first order in BF_3 and 1/2 order in Bu_4NPF_6. This behaviour was rationalized with the following mechanism.

[1] $Bu_4NPF_6 \rightleftarrows Bu_4N^+ +$ 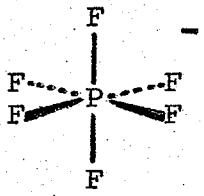

a dissociation of the ion pair Bu_4NPF_6 to the free ions.

[2] 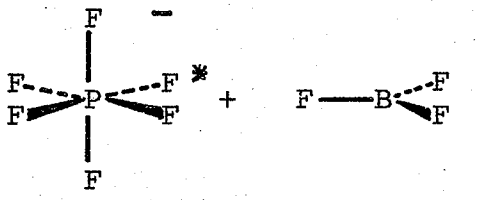

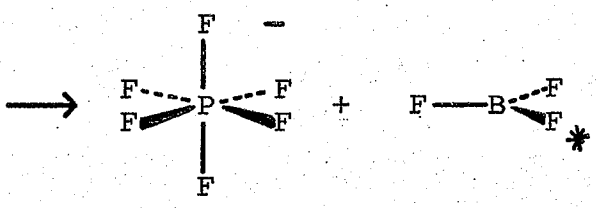

a bimolecular exchange between the PF_6^- ion and BF_3.

If the equilibrium of equation 1 was far to the left, the concentration of free PF_6^- would be proportional to the concentration of the added Bu_4NPF_6 to the 1/2 power. The second step would be a bimolecular exchange between PF_6^- and BF_3, and would be first order in both species. This results in an overall rate process which is 1/2 order in Bu_4NPF_6 and first order in BF_3. Another possibility for the exchange would be:

$$PF_6^- + BF_3 \rightleftharpoons PF_5 + BF_4^-$$

which, if the equilibrium was far to the left, would result in exactly the same nmr lineshape and kinetics as the previous mechanism.

Another group III fluoride exchange that has been studied by an nmr technique is the exchange of aluminum fluorides in aqueous solution.[59] These exchange *via* an intermolecular process, and the following exchange reactions were suggested:

[1] $2\ AlF^{+2} \rightleftarrows Al^{+3} + AlF_2^{+}$

[2] $2\ AlF_2^{+} \rightleftarrows AlF_3 + AlF^{+2}$

[3] $2\ AlF_3 \rightleftarrows AlF_4^{-} + AlF_2^{+}$

All species could be observed in the ^{19}F nmr spectrum and several were observed in the ^{27}Al spectrum. One unfortunate feature of this system, rendering it useless for accurate kinetic studies, is the fairly large quadrupole moment possessed by the ^{27}Al nucleus.

In group IV, no exchange is observed with carbon, but with silicon, exchange is noted in all of the stable coordination numbers. A kinetic study of rapid hydrolysis in $(CH_3)_3SiF$ has been performed by J. A. Gibson in this laboratory.[2,6] The exchange is a rapid hydrolysis, followed by a slow condensation to the siloxane.

[1] $(CH_3)_3SiF + H_2O \rightleftarrows (CH_3)_3SiOH + HF$

[2] $2\ (CH_3)_3SiOH \rightarrow (CH_3)_3SiOSi(CH_3)_3 + H_2O$

The reaction was found to be catalyzed by diethylamine, and the first step was followed by a dnmr technique in which the collapse of the proton magnetic resonance doublet (due to coupling of the fluorine nucleus to the methyl groups) was observed. The Bloch [10] approach was employed to obtain the rate constants from the spectra. The exchange was found to be first order in both $(CH_3)_3SiF$ and diethylamine, and the order with respect to water was 2 at low diethylamine concentrations but dropped to 1 at high concentrations. Furthermore, at high temperatures a negative temperature effect was noted; the exchange rate would actually decrease with an increase in temperature. These results are reminiscent of the the variable solvolysis orders and negative temperature effects found in the hydrolysis and alcoholysis of silicon chlorides,[60] suggesting that perhaps a similarity might exist in the mechanisms. Indeed, alcoholysis of silicon chlorides has been reported to occur with orders with respect to alcohol of up to 7. Several mechanistic possibilities were considered, all of which involve the formation of five or six coordinate intermediates, such as:

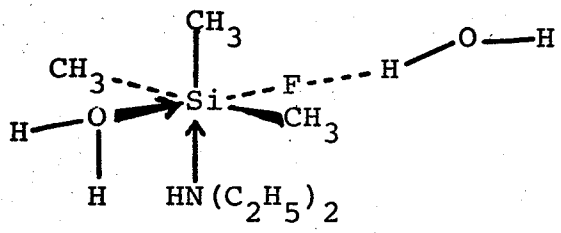

in which one water molecule was envisioned as complexing with the silcon and the other assisted in removing the fluorine. At high diethylamine concentrations the coordinate water could be displaced by another amine, and thereby lower the order in water to 1. Of course, many mechanisms are possible and the dnmr technique does not distinguish one from the rest. It does, however, show the similarity between the reaction of chlorosilanes and fluorosilanes, and much useful kinetic information can be obtained by this technique.

Five coordinate silicon was discussed in chapter 1, and all that can be added here is that both the author and other workers in this laboratory have obtained data that is inconsistent with the previously proposed theories. Addition of a combination drying agent and hydrogen fluoride scavenger (hexamethyldisilazane) was found to inhibit the intermolecular exchange in both SiF_5^- and $CH_3SiF_4^-$.[2,3]

The only six coordinate silicon fluoride that has been studied by a dnmr technique is the $SiF_6^=$ ion. This ion undergoes exchange only under quite acidic conditions, and the mechanism that was postulated (no rate studies were conducted) was:[62]

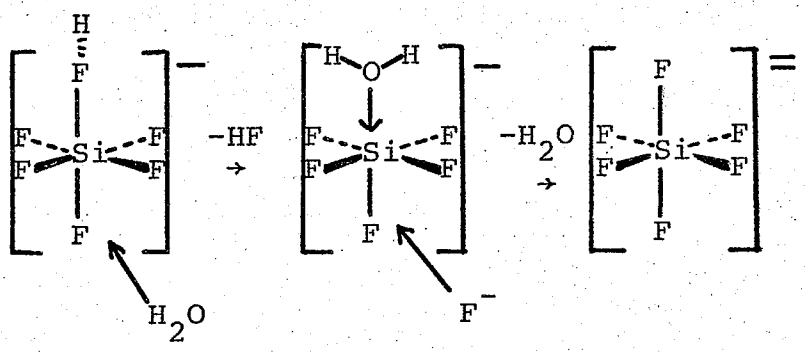

Since all F's are equivalent (octahedral symmetry) no intramolecular exchange process is observable for this species.

In group V, phosphorus provides a profusion of examples of both inter- and intramolecular exchange processes. The intramolecular exchange of a trigonal bipyramid geometry (such as found in phosphorus V compounds) has been recently and thoroughly reviewed.[7] Some very elegant work by Whitesides et al.[63,64] has shown by a dnmr technique that the polytopal rearrangement of fluorines on five coordinate phosphorus proceeds in a manner consistent with the mechanism

originally proposed by Berry [65]

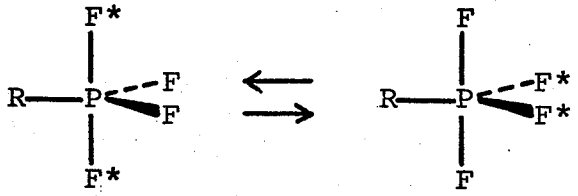

in which both axial and equatorial fluorines exchange in a concerted manner. Intermolecular exchange has also been noted in phosphorus fluorides, generally of the R_3PF_2 and R_4PF types, in which no intramolecular exchange can occur.[7,67] One interesting case is $(CH_3)_2PF_3$, which when first reported was found to exchange in an intermolecular fashion and, when later re-examined by a different group of workers (under conditions of fewer impurities?) was found to undergo only the intramolecular (axial-equatorial) exchange. This example serves to emphasize the role of impurities in these exchanges. Among the other group V fluorides, $(\phi CH_2)_3AsF_2$ has been found to exchange intermolecularly.[70] AsF_5, ϕAsF_4 and ϕ_3BiF_2 all possess very broad ^{19}F nmr resonances and are <u>assumed</u> to undergo an intermolecular exchange of fluorines.[66] Caution must be expressed, however, because ^{75}As, ^{121}Sb, ^{123}Sb and ^{209}Bi all possess sizable quadrupole moments. SbF_5 has been found to be a fluorine bridged polymer in the liquid state.[71-73]

Sulfur tetrafluoride has been shown to exhibit an A_2B_2 ^{19}F nmr spectrum characteristic of a molecule with C_{2v} symmetry, that is, a pseudo-trigonal bipyramid with a lone pair of electrons occupying an equatorial site.[74]

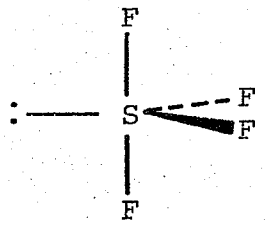

This structure has been confirmed by microwave (pure rotation) spectroscopy [75] and by electron diffraction studies.[76] Cotton et al. proposed a bimolecular intermolecular exchange, inferred from a concentration effect on the rate of exchange. (An impurity catalyzed exchange could also show a similar concentration effect.) In later work,[78] however, they admitted that traces of HF might be responsible for the exchange. Bacon, Gillespie and Quail,[79] as well as the workers in this laboratory, have noted the effect of impurities on the spectrum.[3,84] The early dnmr work [74,77,78] on SF_4 implied an activation energy of about 4 kcal/mol, while the later work on purified samples indicated an activation energy of between 11 and 15 kcal/mol.

This variable activation energy is a suggestion that there might be two mechanisms by which the exchange might occur. These would be: an impurity catalyzed exchange with an activation energy of about 4 kcal/mol, and in the absence of impurities, some other process (intra- or intermolecular) with an activation energy of somewhere between 11 and 15 kcal/mol. Recently, a very thorough (and quite elegant!) dnmr study has been made on SF_4.[82,83] The high energy process was found to be intramolecular, and the mechanism was found to be consistent with Berry pseudorotation.[65] As in the RPF_4 case, the fluorines were found to exchange in a concerted fashion, thus:

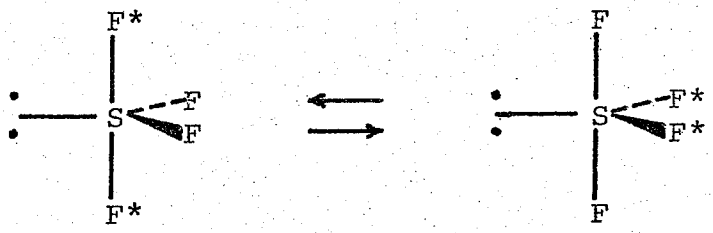

The impurity catalyzed exchange was found to be intermolecular, but no details of the mechanism could be deduced from the dnmr experiment. It should be noted that these experiments required obtaining the ^{19}F nmr spectrum at very low frequencies (6 MHz) in order to make the spectrum as second order as possible. In the RSF_3 series, only the impurity catalyzed intermolecular exchange has been observed;[84,85] the intra-

molecular process presumably is much higher in energy.

Continuing in group VI, R_2SeF_2,[86] SeF_4 [77] and TeF_4[77] have been found to exchange, but the mechanisms are far from clear.

Hydrogen fluoride (included with the halogen fluorides for this discussion) has been found to exchange fluorines at a rate fast enough to cause considerable scaler relaxation of the fluorine nucleus. This exchange is accelerated by trace quantities of water.[87]

Chlorine trifluoride shows an AB_2 ^{19}F nmr spectrum which collapses to a single line at higher temperatures.[88] It is not known whether this is an intramolecular or intermolecular process. The mechanism suggested by Muetterties and Phillips is:

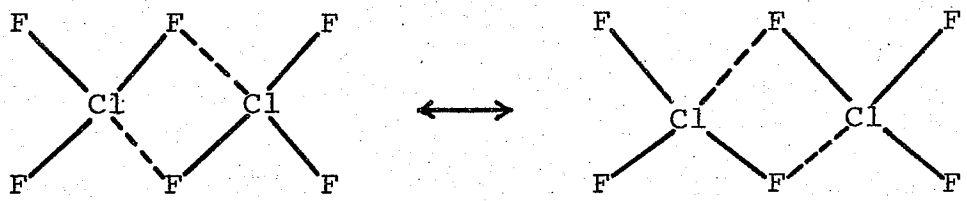

in which the fluorines are transfered via an intermediate fluorine bridged dimer. The exchange has been noted to be impurity catalyzed.[78] Bromine trifluoride was found to exchange in a manner similar to ClF_3.[77] Iodine pentafluoride is the only halogen V fluoride found to exchange, and this occurs only at fairly high temperatures.[21,89]

Of the xenon fluorides, only xenon difluoride and xenon hexafluoride have been found to exchange.[90] This is an intermolecular process monitored by the loss of coupling to the ^{129}Xe nucleus, and occurs only with the addition of hydrogen fluoride as a catalyst. KrF^+ exchanges via an ionization mechanism process in BrF_5 solution.[91]

It can be seen, therefore, that the rapid exchange of fluorines is the rule rather than the exception among the main group inorganic fluorides. Considering the lack of reliable information concerning the mechanism of these exchanges, it is apparent that more work is necessary.

CHAPTER 3 APPLICATION OF THE BLOCH EQUATIONS TO THE PROBLEM OF FLUORINE EXCHANGE IN TETRAPROPYL-AMMONIUM METHYLTETRAFLUOROFILICATE

3.1 The matrix formulation of the Bloch equations

The Bloch approach to the nmr phenomenon is a set of differential equations describing the motion of a macroscopic magnetization $\underline{M}$, in the presence of a stationary magnetic field B_o and an oscillatory field B_1.

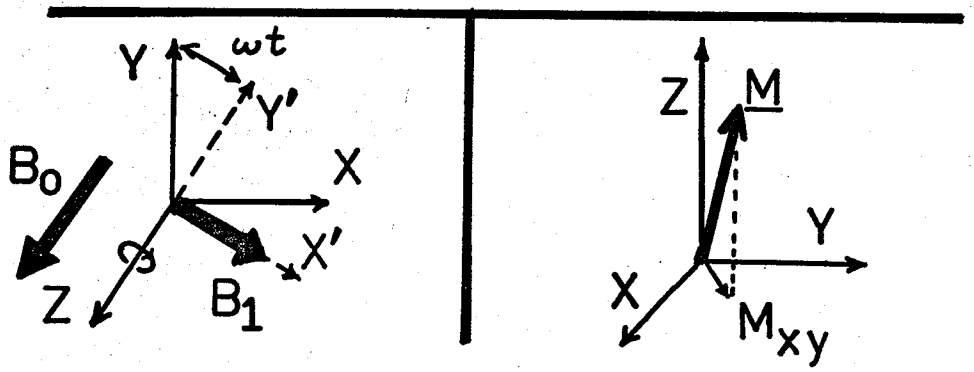

Relationship between the fixed and rotating coordinate frames.

The equation of motion for $\underline{M}$ will be:

$$\frac{d\,\underline{M}}{d\,t} = \gamma \left[M \times (B_1 + B_o)\right] \qquad (3.1)$$

where γ is the magnetogyric ratio for the nucleus involved. Transforming to a coordinate frame rotating at the frequency of the B_1 field, ω, and defining the

component of $\underline{M}$ along the x' axis to be u, and the component along the y' axis to be v, results in the following set of equations:

$$\frac{d\,u_j}{d\,t} = (\omega_j-\omega)v_j - \frac{u_j}{T_{2j}} \qquad (3.2)$$

$$\frac{d\,v_j}{d\,t} = -(\omega_j-\omega)u_j - \frac{v_j}{T_{2j}} - \gamma B_1 (M_z)_j \qquad (3.3)$$

$$\frac{d\,(M_z)_j}{d\,t} = \gamma B_1 v_j - \frac{\{(M_z)_j - M_o\}}{T_{1j}} \qquad (3.4)$$

where T_2 is the time constant for the first order decay of the transverse components of $\underline{M}$ and T_1 is the time constant for the decay of M_z. The subscripts are used to indicate that the nuclei may have several possible Larmor frequencies. $(\omega_j-\omega)$ is the difference in frequency between the j^{th} site and the angular velocity of the rotating frame. The term "site" simply refers to a collection of nuclei with a particular resonance (Larmor) frequency. Reeves and Shaw [15] use the term "nuclear spin isochromat". Equations 3.2 to 3.4 are referred to as the "Bloch equations in the rotating frame".[10]

Since u and v differ only by a 90^o phase relationship, it is usual to combine equations 3.2 and 3.3 into one

complex magnetization G_j: (Analogous to the phasor-locus diagrams in A. C. circuit theory.)[21]

$$Gj = u_j + iv_j$$

$$\frac{d\,G_j}{d\,t} = -(T_{2j}^{-1} + i\Delta\omega_j)G_j - i\gamma B_1 (M_z)_j \qquad (3.5)$$

where $\Delta\omega_j$ is equal to $(\omega_j - \omega)$.

If the nuclei with site frequency ω_j can exchange environments (magnetic, not necessarily chemical) with those of frequency ω_k, a perturbation of the lineshape will occur. McConnell[14] has included this effect into the Bloch equations, and the transverse magnetization in the presence of exchange may be described by:

$$\frac{d\,G_j}{d\,t} = -\left[T_{2j}^{-1} + i\Delta\omega_j + \sum_{k\neq j}\tau_{jk}^{-1}\right] G_j + \sum_{k\neq j}\tau_{kj}^{-1}\, G_j - i\gamma B_1 (M_z)_j . \qquad (3.6)$$

Under steady state conditions all $dG_j/dt = 0$, and if B_1 is made very small so that saturation does not occur:

$$(M_z)_j = P_j M_o$$

where P_j is the population of the j^{th} site and M_o is the equilibrium value of $|\underline{M}|$. τ_{jk} is the mean lifetime before an exchange between site j and k. Therefore:

$$i\gamma B_1 M_o P_j = -\left[T_2^{-1} + i\Delta\omega + \sum_{k\neq j}^{n} \tau_{jk}^{-1}\right] G_j + \sum_{k\neq j}^{n} \tau_{jk}^{-1} G_k \qquad (3.7)$$

There are n of these equations, (one for each site) and each equation contains n unknowns; $G_1, G_2 \cdots G_n$. One solution is by the use of a matrix technique. Equation 3.7, written in matrix form, becomes:

$$i\gamma B_1 M_o \begin{pmatrix} P_1 \\ P_2 \\ \vdots \\ P_n \end{pmatrix} = -\left\{ \begin{pmatrix} R_1 & 0 & \cdots & 0 \\ 0 & R_2 & & \vdots \\ \vdots & & \ddots & 0 \\ 0 & \cdots & 0 & R_n \end{pmatrix} - i \begin{pmatrix} \Delta\omega_2 & 0 & \cdots & 0 \\ 0 & \Delta\omega_2 & & \vdots \\ \vdots & & \ddots & 0 \\ 0 & \cdots & 0 & \Delta\omega_n \end{pmatrix} \right\} \begin{pmatrix} P_1 \\ P_2 \\ \vdots \\ P_n \end{pmatrix} \qquad (3.8)$$

$(R_j = T_{2j}^{-1})$

(cont. on next page)

$$+\left\{\begin{pmatrix} -\tau_{11}^{-1} & \tau_{12}^{-1} & \cdots & \tau_{1n}^{-1} \\ \tau_{21}^{-1} & -\tau_{22}^{-1} & & \\ \vdots & & \ddots & \\ \tau_{n1}^{-1} & & & -\tau_{nn}^{-1} \end{pmatrix}\right\} \begin{pmatrix} G_1 \\ G_2 \\ \vdots \\ G_n \end{pmatrix}, \qquad \text{(3.8, cont.)}$$

Taking transposes of both sides yields: (56)

$$i\gamma B_1 M_o \left(P_1, P_2, \cdots, P_n\right) = \left(G_1, G_2, \cdots, G_n\right)$$

$$\left\{\begin{pmatrix} R_1 & 0 & \cdots & 0 \\ 0 & R_2 & & \\ \vdots & & \ddots & \\ 0 & \cdots & 0 & R_n \end{pmatrix} - i \begin{pmatrix} \Delta\omega_1 & 0 & \cdots & 0 \\ 0 & \Delta\omega_2 & & \\ \vdots & & \ddots & \\ 0 & \cdots & 0 & \Delta\omega_n \end{pmatrix}\right.$$

$$\left. + \begin{pmatrix} -\tau_{11}^{-1} & \tau_{21}^{-1} & \cdots & \tau_{n1}^{-1} \\ \tau_{12}^{-1} & -\tau_{22}^{-1} & & \\ \vdots & & \ddots & \\ \tau_{1n}^{-1} & \cdots & & -\tau_{nn}^{-1} \end{pmatrix}\right\}$$

or, in matrix notation:

$$i\gamma B_1 M_o \underline{P} = \underline{G} (-\underline{R} - i\underline{\Delta\omega} + \underline{K}) \qquad (3.9)$$

where $\underline{P}$ is a row vector of site populations, $\underline{G}$ is a row vector with elements G_j, $\underline{R}$ is a diagonal matrix with elements T_{2j}^{-1} and $\underline{\Delta\omega}$ is a diagonal matrix with elements $(\omega_j - \omega)$. $\underline{K}$ is a rate matrix with diagonal elements $-\tau_{jj}^{-1}$, τ_{jj} being the mean lifetime of a nucleus in site j with resonance frequency ω_j. The off diagonal elements, τ_{jk}^{-1} are the pseudo-first order rate constants for the transfer of magnetization between sites j and k.

Both sides of equation 3.9 may be multiplied by $(-\underline{R} - i\underline{\Delta\omega} + \underline{K})^{-1}$ to give:

$$\underline{G} = i\gamma B_1 M_o \underline{P} (-\underline{R} - i\underline{\Delta\omega} + \underline{K})^{-1} \qquad (3.10)$$

The total sample magnetization, which determines the lineshape, is given by:

$$G = \sum_j^n G_j = \underline{G} \cdot \underline{1}$$

where $\underline{1}$ is a unit column vector. Right multiplication of equation 3.10 by $\underline{1}$ will therefore give an expression for the total transverse magnetization. Thus:

$$G = i\gamma B_1 M_o \underline{P} (-R - i\underline{\Delta\omega} + \underline{K})^{-1} \cdot \underline{1} \qquad (3.11)$$

The absorption mode signal will be the imaginary part of G, since G = u + iv. Multiplying both sides of equation 3.11 by i gives:

$$v = -\gamma B_1 M_o \, \mathrm{Re}\left[\underline{P} \, (\underline{R} + i\underline{\Delta\omega} - \underline{K})^{-1} \cdot \underline{1}\right]$$

where Re means the "real part of". Since spectra are always scaled to a convenient intensity, the constants $\gamma B_1 M_o$ are omitted in the calculation, leaving:

$$v \propto \mathrm{Re}\left[\underline{P} \, (\underline{R} + i\underline{\Delta\omega} - \underline{K})^{-1} \cdot \underline{1}\right] \qquad (3.12)$$

It is interesting to note that a very similar expression has been derived by Sack,[30] based on the work of Kubo and Anderson,[31-34] by treating the exchange problem as a stochastic matrix representation of a Markov probability chain. For this reason the matrix $(\underline{R} + i\underline{\Delta\omega} - K)$ is sometimes referred to as the "Kubo-Sack" matrix, although the method of Kubo and Sack is quantum mechanical and the Bloch approach is classical. The work of Kaplan[24,25] and Alexander[26-29] must also be acknowledged as being a significant contribution to the density matrix theory.

Equation 3.12 could be evaluated as it stands, but this would necessitate the inversion of an n by n matrix for each of several hundred points in the spectrum. However, a method is available that is more efficient

in its use of computer time. The following definition will be made:

$$(\underline{R} + i\underline{\Delta\omega} - K) = (\underline{R} + \underline{\Omega} - \underline{\omega} - \underline{K}) \equiv \underline{A}$$

where $\underline{\Omega}$ is a diagonal matrix with all elements $i\omega_j$ and $\underline{\omega}$ is a diagonal matrix with all elements $i\omega$. $\underline{A}$ may then be divided into a frequency dependent and a frequency independent part, thus:

$$\underline{A} = \underline{B} - \underline{\omega}$$

where $\underline{B} = (\underline{R} + \underline{\Omega} - \underline{K})$.

The inverse of $\underline{A}$ may be obtained by diagonalization of the frequency independent matrix $\underline{B}$.[39,92,93] If the complex matrix $\underline{B}$ can be reduced to diagonal form, $\underline{Bd}$, by some transformation $\underline{U}$, then the same transformation will diagonalize $\underline{A}$.

$$\underline{U}^{-1}\,\underline{B}\,\underline{U} = \underline{Bd}$$

$$\underline{U}^{-1}\,\underline{A}\,\underline{U} = \underline{U}^{-1}\,(\underline{B} - \underline{\omega})\,\underline{U} = \underline{Bd} - \underline{\omega}$$

The inverse of $\underline{A}$ may be found from

$$\underline{A}^{-1} = \underline{U}\,(\underline{Bd} - \underline{\omega})^{-1}\,\underline{U}^{-1}. \qquad (3.13)$$

The inverse of the diagonal matrix $(\underline{Bd} - \underline{\omega})$ may be found by simply taking the reciprocal of the individual elements.

Since $\underline{U}$ was obtained from the frequency independent matrix $\underline{B}$ it will also be frequency independent and hence $\underline{U}$ and $\underline{U}^{-1}$ need only be calculated once per spectrum.

Substitution of equation 3.13 into 3.12 yields the following expression for the v mode magnetization:

$$v \propto \mathrm{Re}\left\{\underline{P}\ \underline{U}\ (\underline{Bd} - \underline{\omega})^{-1}\ \underline{U}^{-1}\ \underline{1}\right\} \qquad (3.14)$$

Following Binsch,[39] the following definitions are made:

$$L_j \equiv \sum_i^n P_i\ U_{ij}\ , \qquad R_j \equiv \sum_k^n U^{-1}_{jk}\ ,$$

$S_j \equiv L_j R_j$ is the so-called "shape vector", and

$Q_j \equiv (Bd_{jj} - \omega)^{-1}$ is the so-called "spectral vector". The spectrum is then computed with the following expression:

$$v \propto \mathrm{Re} \sum_j^n S_j\ Q_j \qquad (3.15)$$

in which a summation is made over each site, j, for a given frequency ω.

It is also convenient to divide the matrix $\underline{K}$ in the following manner:[56]

$$\underline{K} = \underline{p}\ \tau^{-1}$$

where $\underline{p}$ is an n by n probability matrix with diagonal

elements $-p_{jj}$ being the probability that an exchange, chacterized by a mean lifetime, τ, will result in the change of the j^{th} site to some other. The off diagonals, p_{jk}, are the probabilities that site j will become site k after the exchange. It should also be noted that:

$$p_{jj} - \sum_{k \neq j} p_{jk} = 0 \ . \qquad (3.16)$$

In other words, the sum across any row must be zero, and:

$$P_j p_{jj} - \sum P_k p_{kj} = 0 \ , \qquad (3.17)$$

the sum of the elements in any column, when multiplied by the corresponding population, must be zero. Equations 3.16 and 3.17 imply consistency under steady state conditions by making sure that transfers into and out of the j^{th} site are equal.[56]

When described in this manner, the exchange may be described by a single lifetime τ, the inverse of which is a pseudo-first order rate constant. The probability matrix relates the chemical event (exchange of an atom or group of atoms) to the magnetic events (the transfer of magnetization from line to line).

3.2 Matrices and vectors required for the calculation of the exchange broadend proton magnetic resonance spectrum of tetrapropylammonium methyltetrafluorosilicate

Having arrived at a suitable expression for the computation of an nmr spectrum under the influence of an exchange process, it is necessary to provide the various parameters required by the theory. These are: the frequency matrix $\underline{\Omega}$, the population vector $\underline{P}$, the exchange probability matrix $\underline{p}$ and the relaxation matrix $\underline{R}$.

The first step is a careful consideration of the nature of the spectrum itself. All fluorines may be considered to be magnetically and chemically equivalent, due to some type of intramolecular exchange. This will result in (n+1) = 5 lines due to the coupling of the 4 equivalent fluorines to the methyl group, and these lines will have the normal binomial intensity distribution of: (0.0625, 0.250, 0.375, 0.250, 0.0625). Silicon is also known to contain 4.70% of the isotope ^{29}Si, which has a spin angular momentum quantum number of 1/2. This results in a set of low intensity "satellite" peaks separated from the main peaks by $\pm (J_{^{29}Si-^{1}H})/2$. The relative intensity of the satellite and main peaks will be:

(0.0235, 0.953, 0.0235). The spectrum will have, therefore, 15 lines, the intensities of which can be determined by combination of the binomial intensities of the quintet structure and the relative intensities of the ^{29}Si satellite peaks. The $\underline{p}$ vector will then be:

{(0.00140, 0.00561, 0.00842, 0.00561, 0.00140);
(0.0597, 0.2388, 0.3582, 0.2388, 0.0597);
(0.00140, 0.00561, 0.00842, 0.00561, 0.00140)}.

The vector has been divided into blocks of similar silicon spin state, that is:

$\{^{29}Si\text{-}\alpha$; ^{28}Si ; $^{29}Si\text{-}\beta\}$.

This is done in order to provide a block-diagonal form for the probability matrix. (This resulted in a considerable saving in computer time.)

Since the shape of the spectrum depends only on the relative frequencies of the lines, and not on their frequency with respect to some standard, the frequency of the lowest frequency line in the ^{28}Si sub-spectrum is assumed to be 30.0 Hz. The frequencies of all other peaks may be determined with the knowledge that $J_{^{29}Si\text{-}^{1}H} = 9.30$ Hz and $J_{F\text{-}H} = 4.73$ Hz (see Chapter 5). The diagonal $\underline{\Omega}$ matrix, written as a row vector, is therefore:

{(25.35i, 30.08i, 34.81i, 39.54i, 44.27i);
(30.00i, 34.73i, 39.46i, 44.19i, 48.92i);
(34.65i, 39.38i, 44.11i, 48.84i, 53.57i)}

where $i = (-1)^{\frac{1}{2}}$ (recall from section 3.1 that $\Omega_j = i\omega_j$).

All elements of the diagonal relaxatiom matrix, $\underline{R}$, are assumed to be equal, since they are probably determined by inhomogeneity in the magnetic field rather than any "real" relaxation process. The value can be obtained from the width at half height of a non-exchanging line, and the relationship $R_j = (\pi\Delta\nu_{\frac{1}{2}})$.

In order to determine the elements of the transfer probability matrix, it is necessary to study the effect of an intermolecular exchange on the fluorine spin state. Applying the same "commuting Hamiltonian" argument as Shepperd,[94] the effect of spin-spin coupling may be thought of as being equivalent to a magnetic field in the z direction, the methyl protons precessing in one of the 15 possible fields resulting from the combination of silicon and fluorine spin states. The way in which these 15 states result from the 48 possible combinations of states is illustrated in figure (3.1). It is this treatment of spin-spin coupling as a magnetic field (and thus equivalent to a chemical shift) that allows the use of the Bloch equations in a situation in which the sites are determined by coupling. The degenerate states are treated as a single state with an appropriate factor included in the population vector.

M_I	^{19}F spin states	Si isotope and state
5/2	(ααααα)	^{29}Si-α
3/2	(βαααα),(αβααα),(ααβαα),(αααβα)	
1/2	(ββααα),(βααβα),(βαβαα),(αβααβ),(αββαα),(ααββα)	
-1/2	(αβββα),(βαββα),(ββαβα),(βββαα)	
-3/2	(ββββα)	
2	(ααααα)	^{28}Si
1	(βαααα),(αβααα),(ααβαα),(αααβα)	
0	(ββααα),(βααβα),(βαβαα),(αβααβ),(αββαα),(ααββα)	
-1	(αβββα),(βαββα),(ββαβα),(βββαα)	
-2	(ββββα)	
3/2	(ααααα)	^{29}Si-β
1/2	(βαααα),(αβααα),(ααβαα),(αααβα)	
-1/2	(ββααα),(βααβα),(βαβαα),(αβααβ),(αββαα),(ααββα)	
-3/2	(αβββα),(βαββα),(ββαβα),(βββαα)	
-5/2	(ββββα)	

Figure 3.1 The possible states and spin angular momentum quantum numbers resulting from coupling to 4 equivalent fluorine nuclei and a silicon.

Symmeterization of the spin functions has been neglected, and simple product functions are employed to describe the states. These are clearly adequate for the purpose of this work, although they violate the rule of "indistinguishibility of equivalent particles". It should be noted that these functions are all independent, except for the effects of chemical exchange. In other words, the 48 spin states shown in figure 3.1 represent 15 distinct species.

The diagonal elements of the probability matrix are the probabilities that a change of spin state will occur concurrent with an exchange of fluorine nuclei, say $(\alpha\alpha\alpha\alpha) \rightarrow (\beta\alpha\alpha\alpha)$. The probability that the "new" fluorine will have a different spin state than the "old" one will be 1/2, since 1/2 of all the fluorines in the sample will have the α state and the other 1/2 will have the β state. All diagonal elements will therefore be -1/2, the negative sign indicating transfer <u>out</u> of that state. <u>p</u> may then be factored into 3 block-diagonal sub-matrices, corresponding to the ^{28}Si compound and each state of the ^{29}Si compound. This is possible since exchange of a fluorine cannot change the ^{29}Si spin state or change the ^{28}Si into ^{29}Si. The only possible way in which this could occur would be by cleavage of the carbon-silicon bond (exchange of a methyl group) or by a ^{29}Si

Figure 3.2 Diagram of the composite p matrix. Note that there are 3 block-diagonal submatrices corresponding to each spin state of the ^{29}Si isotope and the ^{28}Si isotope. The lines belonging to each row of the matrix are shown to the right of the matrix. The three sets of lines are shown to be separate, while in fact, they overlap.

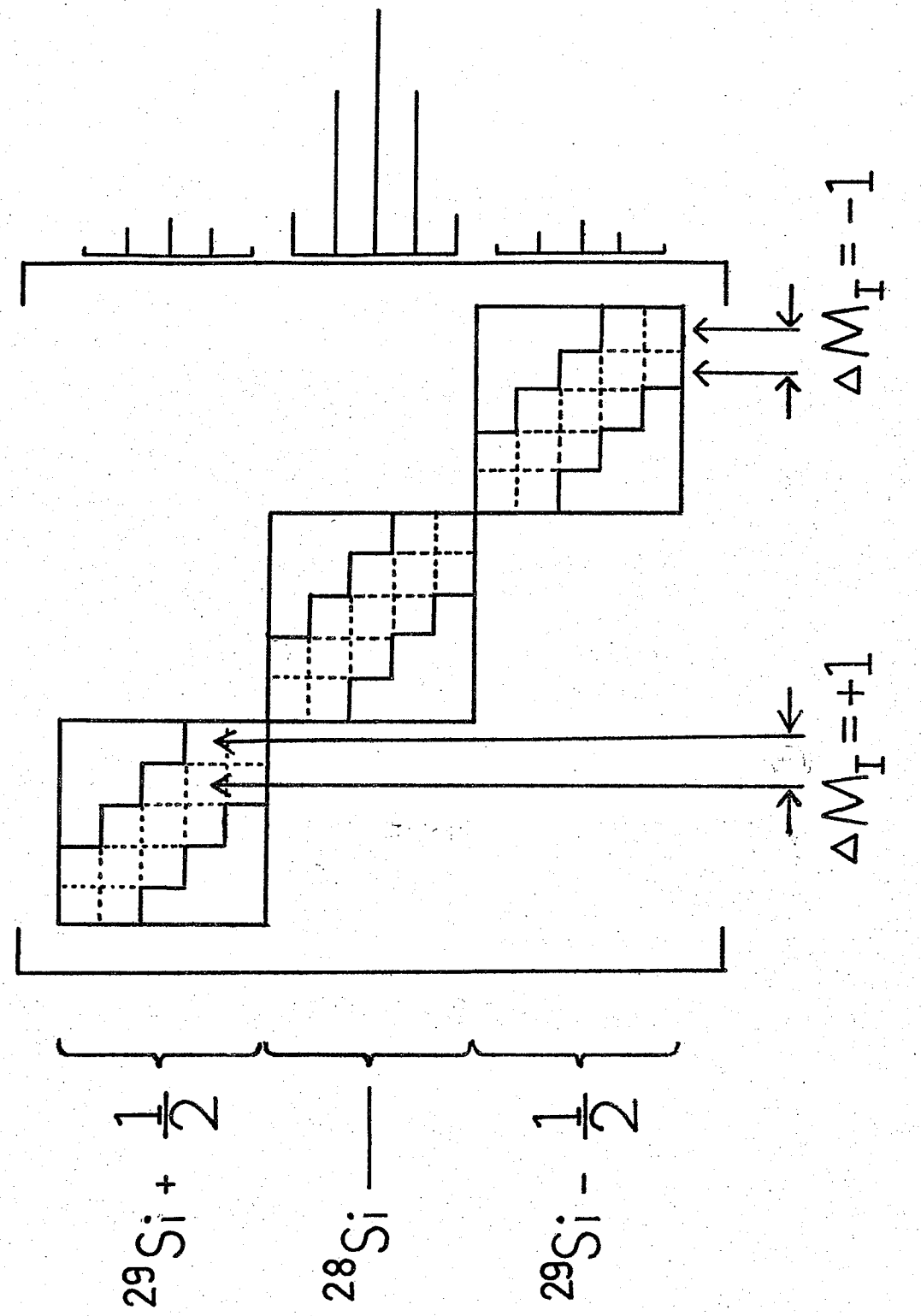
$\Delta M_I = -1$
$\Delta M_I = +1$
$^{29}Si^{+}_{\frac{1}{2}}$
^{28}Si
$^{29}Si^{-}_{\frac{1}{2}}$

Figure 3.3 One of the blocks of the p matrix. The elements are determined by methods described in the text. Note that the only non-zero elements are on the diagonal and the first supra- and superdiagonals.

Each row of the matrix represents one line of the slow exchange spectrum, while each column represents the line(s) to which magnetization may be transfered during exchange. The matrix element corresponding to this row and column is the probability that magnetization will be transferred between those two lines during a chemical exchange.

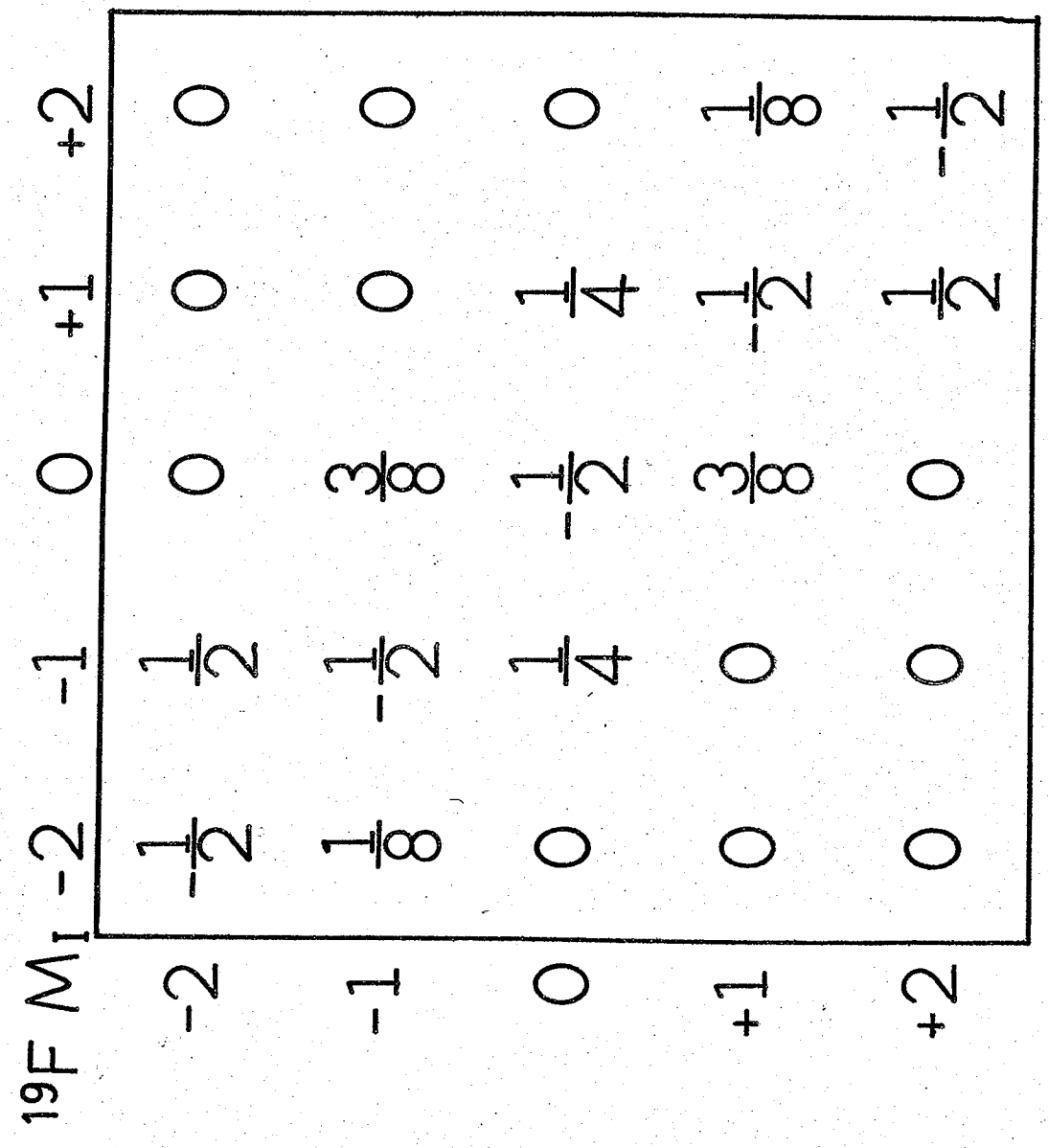
^{19}F M_I
-2
-1
0
+1
+2
-2 -1 0 +1 +2
-2 -1/2 1/8 0 0 0
-1 1/2 1/2 1/4 0 0
0 0 3/8 1/2 3/8 0
+1 0 0 1/4 1/2 1/2
+2 0 0 0 1/8 1/2

T_1 relaxation process. Methyl transfer can be ruled out since the ^{29}Si-CH_3 coupling is maintained even at the highest fluorine exchange rates observed in this work. Furthermore, ^{29}Si relaxation times are known to be long.[95] When the $\underline{P}$ vector, the $\underline{\Omega}$ matrix and the $\underline{R}$ matrix are similarly blocked the problem is reduced to the summation of three separate 5-line spectra and the the diagonalization of three 5 by 5 matrices rather than a 15 by 15 matrix. This results in a considerable reduction of computer time and improves the accuracy of the results. A schematic diagram of the composite $\underline{p}$ matrix is shown in figure 3.2.

Each 5 by 5 block of the probability matrix will be identical, the fluorine exchange probabilities being independent of the silicon isotope or state. A detailed calculation will be carried out only for the ^{28}Si sub-matrix.

As previously stated, all diagonal elements are -1/2. It should be noted that the exchange of a fluorine will result in a change in the total spin angular momentum quantum number, M_I, of 0 or ±1 depending on whether the new fluorine has the same or opposite spin state as the old one. For chemical reasons, the probability of a simultaneous exchange of two fluorines is considered slight. Therefore, all off-diagonals are

zero except for those on the first supra- and superdiagonals. The matrix element corresponding to line i becoming line j is represented by p_{ij}. The lines of the ^{28}Si sub-spectrum are represented by the indices 6 to 10 inclusive, corresponding to the M_I values of -2 to +2. Each row in the $\underline{p}$ matrix may be thought of as representing one line in the non-exchanging spectrum. The columns correspond to the lines to which magnetization may be transferred after the exchange. $p_{6,7}$ therefore, is the probability that the nuclei corresponding to line 6 will have the resonance frequency of line 7 after the exchange. This is the only off-diagonal in the sixth row, and from the condition that the sum across a row must be zero, $p_{6,7} = 1/2$. The seventh row of the matrix (second row of the sub-matrix) will have two off-diagonal elements, $p_{7,6}$ and $p_{7,8}$. From equation 3.16

$$p_{7,6} + p_{7,8} = 1/2,$$

and from equation 3.17

$$\frac{1}{16} p_{6,6} + \frac{1}{4} p_{7,6} = 0.$$

Since $p_{6,6} = -1/2$, $p_{7,6} = 1/8$ and $p_{7,8} = 3/8$. The eighth row of the matrix also has two off diagonals, $p_{8,7}$ and $p_{8,9}$. From the symmetry of the spectrum and equation 3.16 $p_{8,7} = p_{8,9} = 1/4$. Similarly $p_{9,8} = 3/8$, $p_{9,10} = 1/8$ and $p_{10,9} = 1/2$. The complete sub-matrix is shown in figure 3.3.

Figure 3.4 shows the effect of τ on the spectrum.

Figure 3.5, on the other hand, shows the effect of the transverse relaxation time, T_2. Note that the effects on the lineshape are slightly different, and under favourable circumstances the effects may be separated.

Figure 3.4 The effect of the pre-exchange lifetime on the spectrum. The transverse relaxation time, T_2, was set at 1.0 sec. The arrows point out the position of the silicon 29 satellite peaks.

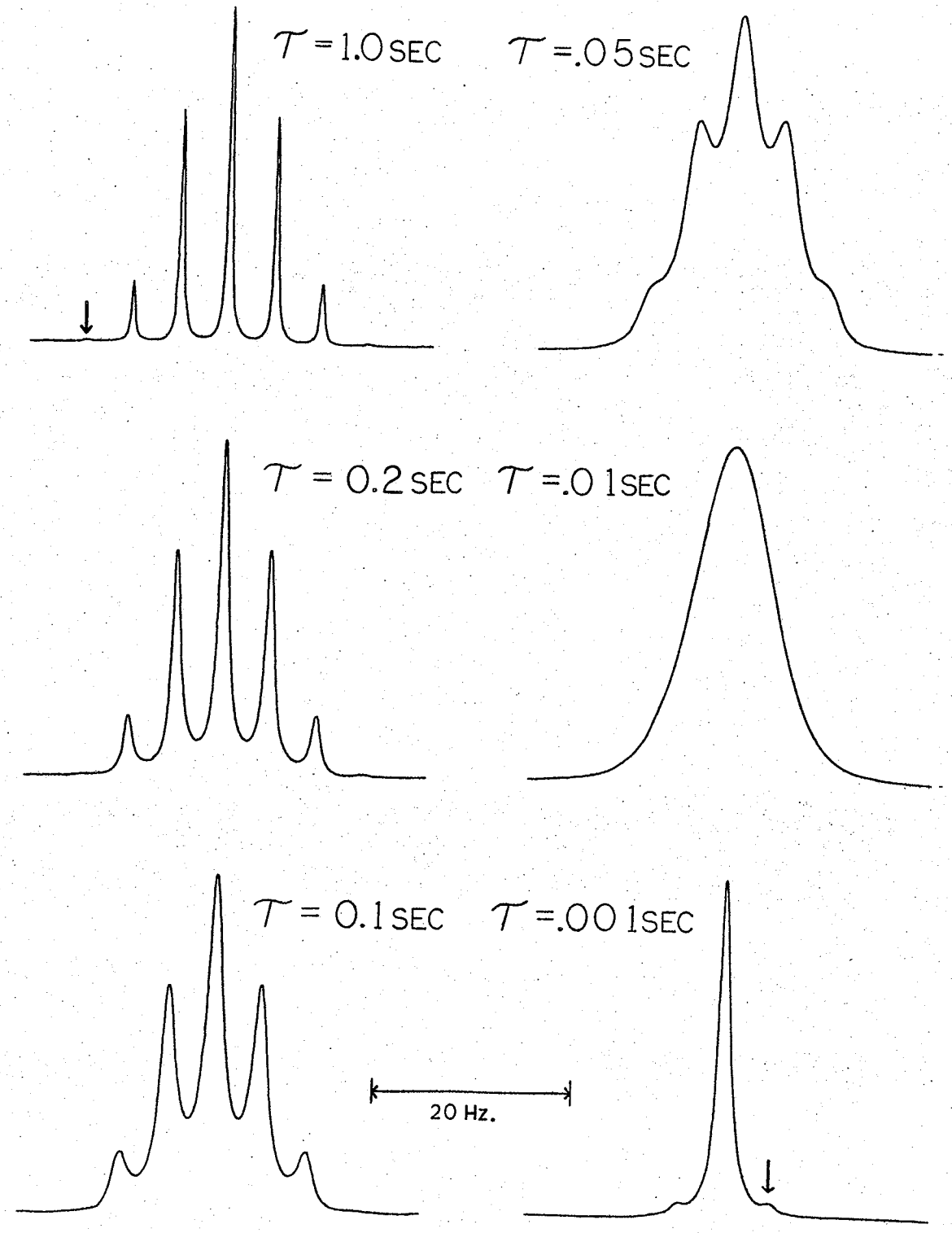
τ = 1.0 SEC
τ = .05 SEC
τ = 0.2 SEC
τ = .01 SEC
τ = 0.1 SEC
τ = .001 SEC
20 Hz.

Figure 3.5 The effect of the transverse relaxation time on the spectrum. The peak becomes broader as the relaxation time becomes shorter.

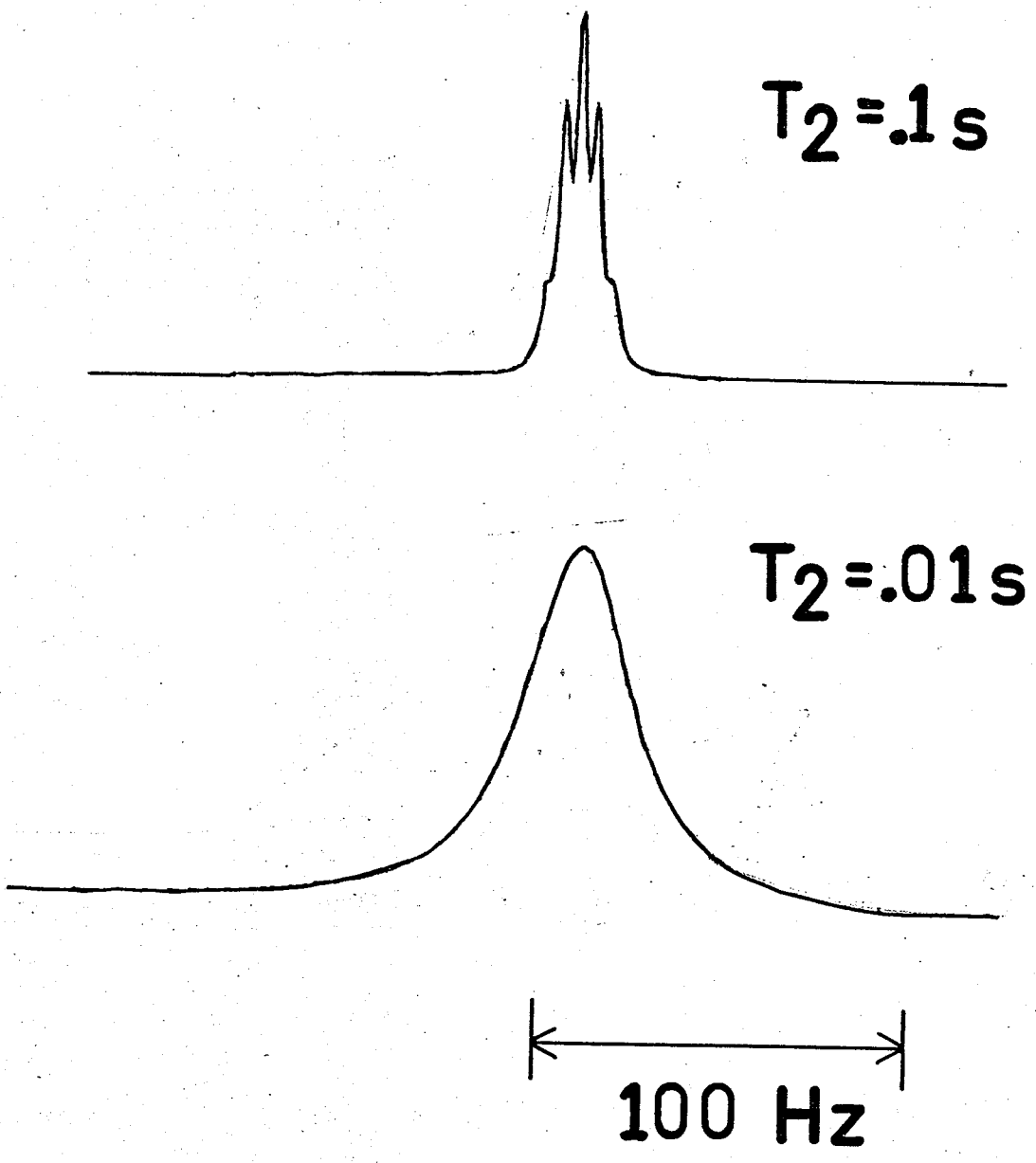
T_2=.1 s
T_2=.01 s
100 Hz

3.3 Relationship between the dnmr technique and chemical kinetics

The dynamic nuclear magnetic resonance technique essentially measures the mean lifetime τ, of a species, A, observed at equilibrium. This lifetime can be related to the macroscopic reaction rate, $d[A]/dt$, by:[58,95,96]

$$(f_A \tau_A) = \frac{[A]}{d[A]/dt} \qquad (3.18)$$

where f_A is a statistical factor relating the lifetime of the species being observed to the lifetime of the nucleus being exchanged.[58,96,97] This is necessary because the mathematical technique employed to generate the spectra mixes all of the lines at a rate of τ^{-1}, but the exchange of a single nucleus can only mix any pair of the lines (since $\Delta M_I = \pm 1$). In the case of the $CH_3SiF_4^-$ ion, this factor will be 1/4 because there are four fluorines which can undergo exchange, and exchange of any one of them will result in the mixing of any one of the $\Delta M_I = \pm 1$ pairs. In an intermolecular exchange of a spin 1/2 nucleus where the exchange is followed by the loss of coupling to the nucleus being exchanged, there is an additional factor of 1/2 due to the fact that there is an even chance that the incoming nucleus will have the same spin state as the one that left (a 50% probability that $\Delta M_I = 0$). This is an

ineffectual exchange as far as the dnmr experiment is concerned, even though a chemical event has occurred. One or both of these factors may be combined into the exchange probability matrix, described in sections 3.1 and 3.2.†

The usual general form of a chemical rate expression is:

$$\frac{d[A]}{dt} = k\,[A]^{x}\,[B]^{y} \quad . \quad . \quad . \quad . \qquad (3.19)$$

where k is the specific reaction rate constant. Combining equations 3.18 and 3.19 gives:

$$(f\tau)^{-1} = k\,[A]^{x-1}\,[B]^{y} \quad . \quad . \quad . \quad . \qquad (3.20)$$

which, for the methanol catalyzed fluorine exchange in $CH_3SiF_4^-$, becomes:

$$\tau^{-1} = \frac{1}{4}\,k\,[CH_3SiF_4^-]^{x-1}\,[CH_3OH]^{y} \qquad (3.21)$$

A convenient method for the determination of the kinetic orders, x and y, is to make a plot of $\ln(\tau^{-1})$ as a function of ln(concentration). For example, if the order with respect to $CH_3SiF_4^-$ is required, the methanol concentration would be held constant and equation 3.21

---

† In this work, the factor of 1/2 was explicitly combined into the exchange probability matrix, while the factor of 1/4 was not.

could be written:

$$\ln (\tau^{-1}) = (x-1) \ln [CH_3SiF_4^-] + \ln\left[\frac{1}{4} k [CH_3OH]^y\right] \quad (3.22)$$

which is a linear function with a slope of (x-1) from which the order may be obtained. If the $CH_3SiF_4^-$ concentration is held constant and the methanol concentration is varied, the logarithmic form of equation 3.21 will be:

$$\ln (\tau^{-1}) = y \ln [CH_3OH] + \ln\left[\frac{1}{4} k [CH_3SiF_4^-]^{(x-1)}\right] \quad (3.23)$$

which will have a slope of y.

Equation 3.21 may also be solved for k:

$$k = \frac{4}{[CH_3SiF_4^-]^{x-1} [CH_3OH]^y \tau} \quad (3.24)$$

The standard treatments can be used to gain information about the activation thermochemistry of the process. Since [95]

$$k = A_o \exp(-E_a/RT)$$

$$\ln k = \ln A_o - \frac{E_a}{RT} \quad (3.25)$$

and a plot of ln k as a function of 1/T will have a slope of -Ea/R, yielding the activation energy. It is possible knowing k and E_a, to obtain other thermodynamic values, since:

$$k = \frac{k_b}{h} \exp(\Delta S^{\dagger}/R) \cdot \exp(-E_a/RT) \qquad (3.26)$$

it is possible to obtain a value for the activation entropy ($\Delta S^{\dagger}$), and since [95]

$$\Delta G^{\dagger} = \Delta H^{\dagger} - T\,\Delta S^{\dagger}$$

and

$$\Delta H^{\dagger} = E_a - RT$$

it is possible to obtain values for the activation enthalpy ($\Delta H^{\dagger}$) and the free energy of activation ($\Delta G^{\dagger}$).

CHAPTER 4 EXPERIMENTAL

4.1 Materials

Methyltrifluorosilane and 2,6-di-(2-methylpropyl)-pyridine were obtained from PCR, inc. and were used without further purification. Tetrapropylammonium hydroxide was obtained from the Eastman Kodak Co. as a 10% solution in water. Antimony trifluoride, methyltrichlorosilane and hydrofluoric acid were obtained from the Fischer Scientific Co. Ltd. and were used without further purification. Methanol was treated with sodium and distilled under vacuum while pyridine was treated with "Linde" (Union Carbide Co. Ltd.) 3A molecular sieve. Methylene chloride was distilled under vacuum from phosphorus pentoxide and stored over 3A molecular sieve prior to use in NMR samples. 1,2-Dimethoxyethane was found to contain large quantities of water and was poured through a column of 3A molecular sieve, followed by distillation from lithium aluminum hydride. Direct treatment of 1,2-dimethoxyethane with lithium aluminum hydride resulted in several fires.

4.2 Instrumental

All proton magnetic resonance spectra were recorded on

a Varian HA-100-D spectrometer at 100 MHz. The solvent resonance (CH_2Cl_2) was employed for field/frequency stabilization in the frequency-sweep mode. Frequencies were measured with a Hewlett-Packard 5323A frequency counter and are reported in Hz to high field of the solvent resonance. These frequencies are considered accurate to ±0.02 Hz. The proton resonance from natural abundance $^{13}CH_2Cl_2$ provided a convenient signal for monitoring the "natural" linewidth of the spectrometer, thus giving a value for T_2. The strength of the R.F. field B_1 was 0.025 mG as determined by the method of Harris and Worvill.[98] Spectra run with a field strength of three times this value showed negligible distortion due to saturation effects. Spectra were recorded at a sweep width of 2 Hz/cm at a sweep rate of 0.1 Hz/s. Filtering of the signal was restricted to the minimum amount required for a reasonable signal to noise ratio.

Sample temperatures were determined with an iron-constantan thermocouple placed at sample depth in a "dummy" sample of methylene chloride. Temperatures are considered accurate to ±1° C.

Wilmad 503-PS precision ground sample tubes were employed for all studies reported in this thesis. These tubes were chosen for their reproducible spinning characteristics. Sample spinning rates were fast enough to en-

sure that spinning sidebands would not overlap any part of the spectrum.

Fluorine nuclear magnetic resonance spectra were recorded on a modified Varian DA-60-IL spectrometer at 56.443 MMz, again in the frequency-sweep mode. 1,1,1-Trifluoro-2,2,2-trichloroethane was used as the "lock" signal, and all reported frequencies are to high field of this resonance. Frequency and temperature calibrations were performed in the same manner as on the HA-100-D.

Infrared spectra were recorded on a Perkin-Elmer 337 grating spectrophotometer.

A Finnigan 1015 quadrupole mass spectrometer provided the mass spectra for this work. The energy of the electron impact beam was 70 eV.

4.3 Preparation of Tetrapropylammonium Fluoride

Tetrapropylammonium hydroxide (25 ml of a 10% solution) was diluted to 3% and neutralized to a pH of 7 with dilute hydrofluoric acid. The neutralization was monitored with a glass electrode pH meter of standard design. The resulting solution was reduced to a thick oil on a rotary evaporator. Methanol (100 ml) was added and the solution was again evaporated to the point of being a thick oil. This procedure of adding methanol followed by evaporation was

repeated three times in an effort to remove as much of the water as possible. The solution was then evaporated to dryness under a vacuum of 10^{-3} torr at 100^{o} C. The resulting 2.7 g of white powder was found to be very hygroscopic and was handled in a dry-box at all times.

4.4 Preparation of Methyltrifluorosilane

Antimony trifluoride (30 g, .17 mole) and 25 g of benzene were placed in a 75 ml stainless steel reaction cylinder and cooled to -78^{o} C. 15 g (0.10 mole) of methyl trichlorosilane was added. The cylinder was then sealed with a stainless steel valve and evacuated. After allowing the reaction to proceed at room temperature for 24 h, the volatile materials were separated by "trap-to-trap" distillation on a conventional "pyrex" vacuum system. The traps were maintained at -78^{o} C, -120^{o} C and -196^{o} C; the desired product was collected at -120^{o} C. The 6.7 g (79% yield) of the product was then condensed into another stainless steel cylinder.

Mass spectrometric investigation indicated that the correct product had been formed, with a few low intensity peaks at higher mass. These peaks could not, however, be readily identified. The proton magnetic resonance spectrum had the expected quartet with a few low intensity (<1%,

total proton count) impurity peaks.

4.5 Preparation of Tetrapropylammonium Methyltetrafluorosilicate

Tetrapropylammonium methyltetrafluorosilicate was prepared by a method similar to that of Klanberg and Muetterties.[1] Tetrapropylammonium fluoride (1 g, 4.88 mmole) was placed in a glass reaction tube along with 5 ml of methanol. The tube was attached to a vacuum line via a ground glass joint, evacuated, and cooled to -196°C. Commercial (PCR) methyltrifluorosilane (0.67 g, 6.7 mmole) was condensed into the tube from the vacuum line and the tube was flame sealed at -196°C. The reaction mixture was allowed to warm to room temperature and gaseous materials, mainly excess CH_3SiF_3, were vented into the vacuum system. The resulting methanol solution of tetrapropylammonium methyltetrafluorosilicate was filtered through a fine sintered glass disc into a 100 ml round-bottom flask. The addition of 20 ml of anhydrous ether resulted in the formation of a white precipitate which, after cooling to ∿ -30°C, was collected by vacuum filtration under a blanket of dry nitrogen. This precipitate was recrystallized from ∿15 ml of 1,2-dimethoxyethane and washed with diethyl ether. The yield was 0.7 g (47%) of

white needle-like crystals, melting point 157 - 159°C (literature, 161 - 164°C [1]).

Repeating the reaction with the methyltrifluorosilane prepared in this laboratory resulted in a total failure to produce tetrapropylammonium methyltetrafluorosilicate with the required purity. The product from the reaction of the fluorosilane produced in this laboratory was a granular hygroscopic material, rather than the crystals characteristic of the desired product. The proton magnetic resonance spectrum (CH_2Cl_2) showed a set of peaks characteristic of the tetrapropylammonium ion, and a single peak at the expected resonance frequency of the methyl group in the $CH_3SiF_4^-$ ion. The fact that this was a single peak rather than a five line multiplet, indicated that a rapid exchange process was occurring, suggestive of a high impurity level. Integration of the spectrum showed that this peak had only 24% of the required intensity, based on the intensity of the tetrapropylammonium peaks. The material was thus assumed to only 24% product and 76% of some other tetrapropylammonium salt, probably tetrapropylammonium fluoride. Infrared spectroscopy indicated the presence of water in the material. Numerous attempts to purify the methyltrifluorosilane by "trap-to-trap" distillation again resulted in material unsuitable for the preparation of tetrapropylammonium methyltetrafluoro-

silicate.

The source of this problem was never determined. However, several impurity peaks with isotope distribution characteristic of double chlorine substitution always occurred in the mass spectrum of the CH_3SiF_3 prepared by the author. (m/e = 133 and m/e = 148) These peaks were absent in the commercial product. This fact is interesting when one considers that Klanberg and Muetterties [1] have noted that commercial tetraalkylammonium fluorides contaminated with chloride ion were unsuitable for the preparation of tetraalkylammonium fluorosilicate salts.

4.6 Vapour pressure molecular weight determination

The vapour pressure of pure methylene chloride and a 0.6 mol l^{-1} solution of tetrapropylammonium methyltetrafluorosilicate in methylene chloride were determined at 25°C with the aid of a mercury manometer attached to a pyrex vacuum manifold. A direct application of Raoult's law yielded an effective molecular weight of 330 ± 20 g mol^{-1}. [99]

4.7 Preparation of the nmr samples

The precision bore 5 mm sample tubes were calibrated

to contain exactly 0.3 or 0.5 ml of liquid by the use of a small volume syringe. These calibration points were then scratched into the surface of the glass. The tubes were then cleaned with methylene chloride, treated with hexamethyldisilazane to remove any traces of moisture, and dried at 220^{o}C for at least 24 h.

The required ammount of tetrapropylammonium methyltetrafluorosilicate was then weighed into the sample tube, methanol (and, for some experiments, pyridine or 2,6-di-(2-methylpropyl)-pyridine) was added by a gas chromatographic type of "micro syringe", and the total volume was made up to the required calibration mark with methylene chloride. The tube was then capped, sealed with "teflon" tape, and inverted several times to ensure thorough mixing.

In order to reduce the number of samples required, the same sample was sometimes used for several runs at different concentrations. This was accomplished by removing the sample from the spectrometer probe, warming the sample to room temperature (if the sample had been cooled), opening the sample and injecting in a measured volume of methanol (or pyridine or 2,6-di-(2-methylpropyl)pyridine). After thorough mixing the spectrum was again recorded. The volume added (5 - 10 µl) was always very small compared to the total sample volume (0.3 or 0.5 ml) so that the error due to volume change on mixing was always

less than 3%. Since the estimated error in the lineshape analysis is in the order of 10%, this was ignored. Samples were equilibrated for at least 20 min at probe temperature, and concentration changes due to volume variations with temperature were also ignored.

Samples for the determination of activation energies and entropies were flame sealed under dynamic vacuum and stored in liquid nitrogen when not in use. This was found to be necessary in order to avoid the deleterious effects of sample aging.

4.8 Comparison of calculated and experimental spectra

All calculated spectra were produced with a modified version of the computer program "EXCHSYS" obtained by Dr. L. J. Kruczynski from Dr. G. M. Whitesides' group at MIT. Since this program was set up in the density matrix formalism some modification was necessary to use the program for the Bloch method. Most of these modifications involved the removal of unnecessary parts of the program. Matrix diagonalization and inversion routines were identical to those employed by G. Binsch in the program "DNMR3".[43]

The computations were performed with an IBM 370-158-KJ computer and the "fortran" H level compiler. The

digital output from the computer was plotted on a Calcomp 750/563 or Versatec D1200-A plotter.

Due to the large number of spectra that had to be compared and the high symmetry of the spectra, a numerical procedure was employed for comparison of the spectra. For spectra past the point of coalescence, the half-height width of the experimental spectrum was compared to a graph of half-height width as a function of τ^{-1}. Graphs of this type were made for a number of different T_2 values. The T_2 values for the experimental spectra were obtained from the half-height width of the $^{13}CH_2Cl_2$ peak. For spectra at slower exchange rates, graphs were prepared of "valley to peak" ratio as a function of τ^{-1} for a range of T_2 values. Spectra at intermediate exchange rates were analyzed by direct visual comparison with the calculated ones. Figures 4.1 to 4.3 illustrate these measurements.

Values determined by this method were considered accurate to ±10%.

Figure 4.1 The measurements used to produce the calibration graphs shown in figures 4.2 and 4.3.

A The valley-to-peak ratio is the value V/P, and is independent of absolute height of the spectrum.

B The half-height width of an exchange averaged Lorentzian peak.

A

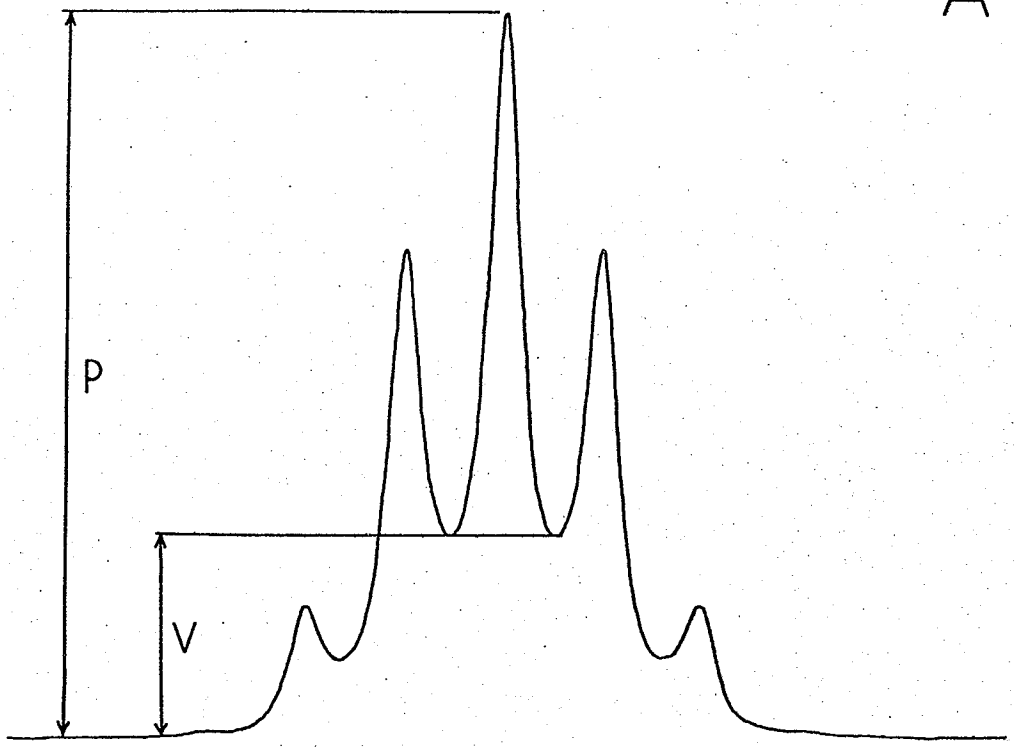

B

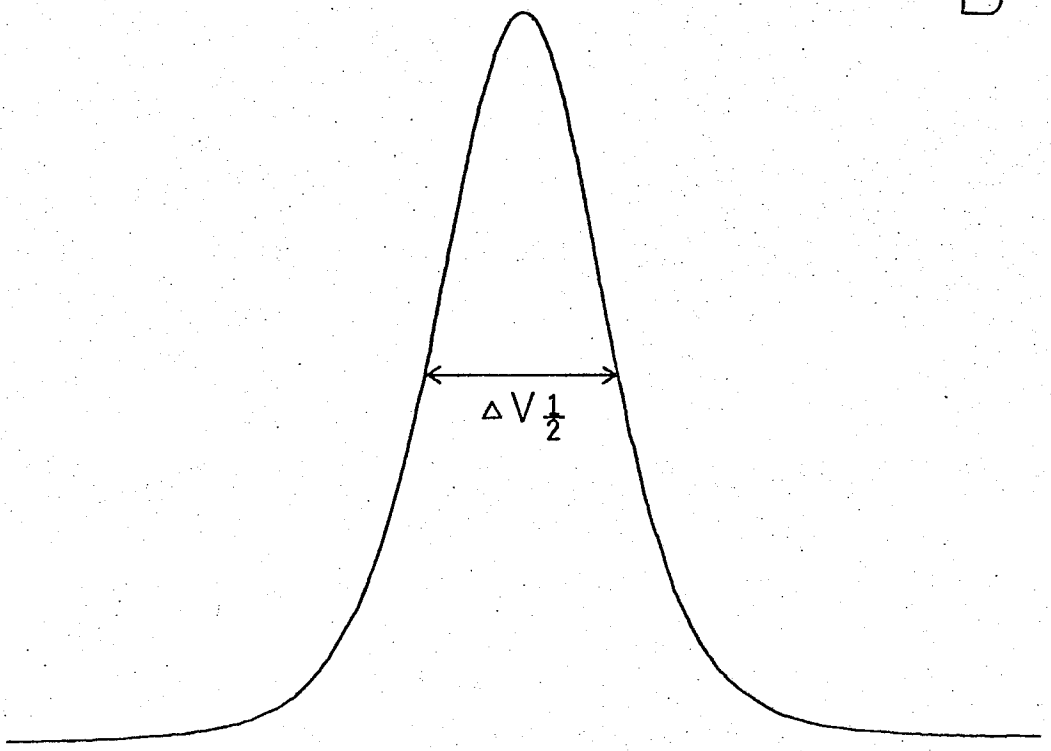

Figure 4.2 A calibration graph for spectra that still show fine structure (multiplet splitting). The valley-to-peak ratio is plotted as a function of exchange rate.

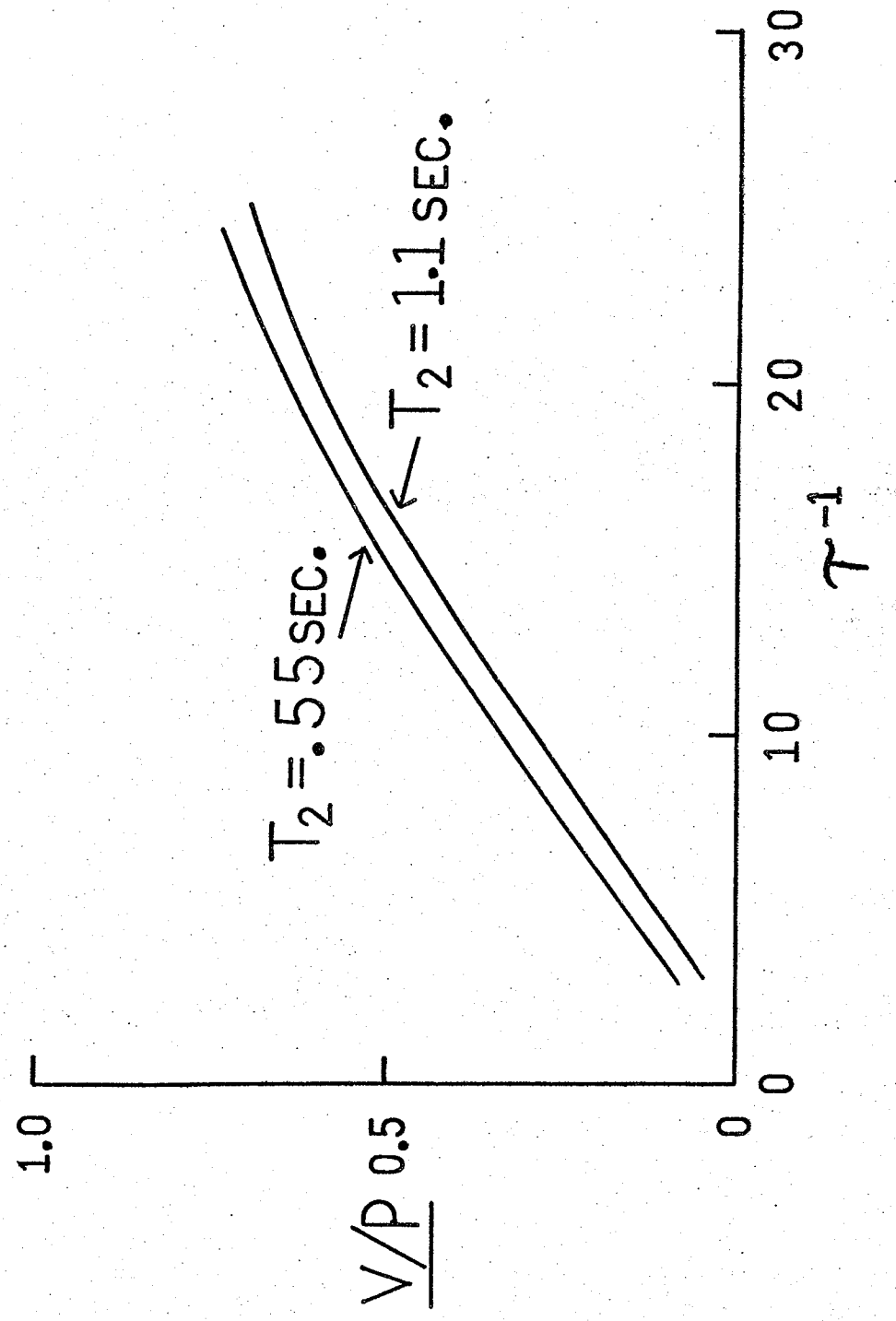
1.0
0.5
V/P
0
10
20
30
τ-1
T2 = .55 SEC.
T2 = 1.1 SEC.

Figure 4.3 A calibration graph for spectra past the point of coalescence. The half-height width of the single peak is plotted as a function of exchange rate.

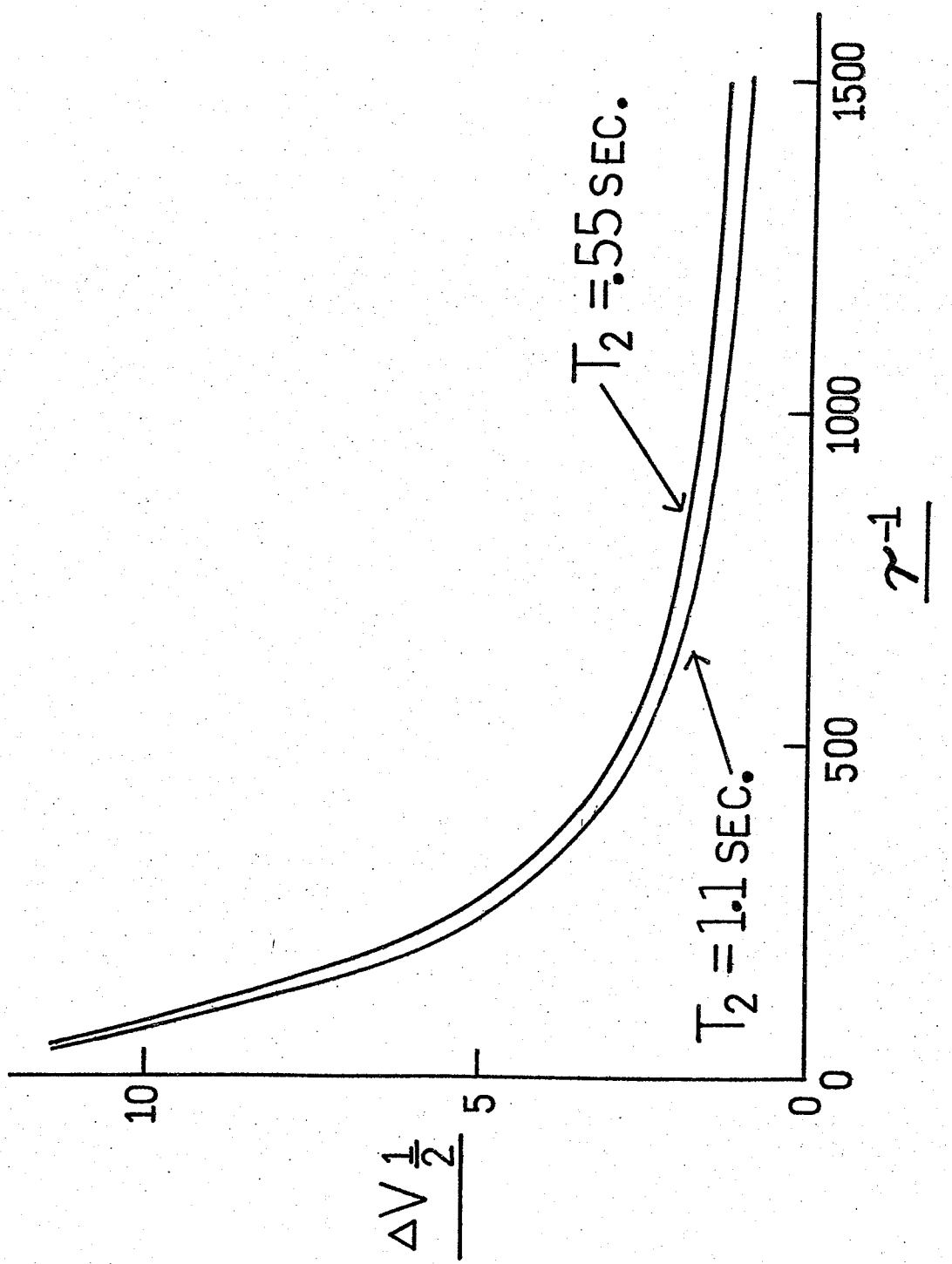
$\Delta V_{\frac{1}{2}}$
10
5
0
0
500
1000
1500
τ^{-1}
$T_2 = .55$ SEC.
$T_2 = 1.1$ SEC.

CHAPTER 5 RESULTS

5.1 Determination of the fluorine-hydrogen coupling constant, $J(^{19}F-^{1}H)$

The fluorine-hydrogen coupling constant was determined with a sample containing 100 mg of tetrapropylammonium methyltetrafluorosilicate in 0.5 ml of methylene chloride (0.66 mol l^{-1}) at 31.5°C (ambient probe temperature). The value obtained was 4.73 ± 0.05 Hz, the reported uncertainty being the standard deviation in 12 measurements (three spectra, four splittings per spectrum). The coupling constant was also measured at -60°C with a sample containing 60 mg of tetrapropylammonium methyltetrafluorosilicate in 0.3 ml of methylene chloride (0.66 mol l^{-1}), and 25 µl (1.98 mol l^{-1}) of methanol. The value obtained under these conditions was 4.81 ± 0.10 Hz, the uncertainty being the standard deviation in 12 measurements. The somewhat larger standard deviation probably is the result of the slightly broadish nature of the peaks under these conditions ($\Delta\nu_{\frac{1}{2}}$ = 0.5 Hz). This change in the coupling constant amounts to only 1.7% in a 90° temperature change, and was ignored. Since most spectra were recorded at or near the ambient temperature, the value of 4.73 Hz was used in

all calculations.

5.2 Determination of the silicon-hydrogen coupling constant, $J(^{29}Si-^{1}H)$

The silicon-hydrogen coupling constant was determined with a sample containing 100 mg of tetrapropylammonium methyltetrafluorosilicate in 0.3 ml of methylene chloride (1.1 mol l^{-1}) at -20°C. Due to overlapping of the main and satellite peaks it was possible to determine the coupling constant from the outermost (lowest intensity) lines only. This necessitated the use of high B_1 levels, high gain and extreme damping of the resultant signal. The result obtained under these conditions was 9.3 ± 0.2 Hz. No isotope shift was noted.

5.3 The effect of methanol concentration on the exchange rate

Samples were prepared with varying methanol concentrations, as described in section 4.7. A natural log plot of τ^{-1} as a function of methanol concentration is shown in figure 5.5; the data used to produce this graph are shown in table 5.1. The concentration of tetrapropylammonium methyltetrafluorosilicate was 0.66 mol l^{-1}. A

least mean squares analysis of the data yielded a slope, and hence the order with respect to methanol, of 1.95 ± 0.09. Within experimental error, the kinetic order with respect to methanol is 2 (see equation 3.23).

5.4 The effect of tetrapropylammonium methyltetrafluorosilicate concentration on the exchange rate

The exchange rate of this compound shows a most remarkable negative concentration dependence. It can be seen from the data in table 5.2 that the exchange rate actually increases with a decrease in concentration. Natural log plots of τ^{-1} as a function of tetrapropylammonium methyltetrafluorosilicate concentration are ahown in figure 5.2. The slopes of the lines (least squares) are: -17°C, -1.5± 0.2; -25°C, -1.2 ± 0.2, -1.2 ± 0.1. The difference in the position of the two lines at -25°C may be attributed to an error in methanol concentration, or a drift in the temperature calibration of the HA-100 spectrometer. The latter condition was noted on several occasions, particularly in the temperature range from 0°C to -30°C whenever liquid nitrogen was employed as a coolant. In later studies it was found that a "dry ice"/acetone mixture provided much better stability under these circumstances.

Since the observed order is one less than the true

kinetic order (equation 3.22), the order with respect to tetrapropylammonium methyltetrafluorosilicate is between -0.2 and -0.5 in this temperature range.

5.5 The effect of pyridine on the exchange rate

The effect of the typical Lewis base, pyridine, is shown in figure 5.3 and table 5.3. The line is reasonably linear with a slope of -0.5 ± 0.1 (least squares) until a concentration of about 1 mol l^{-1}, at which point the slope becomes steeper, approaching a value of -1. The sample temperature was 31.5°C; the methanol concentration was 1.0 mol l^{-1}, and the tetrapropylammonium methyltetrafluorosilicate concentration was 0.66 mol l^{-1}.

5.6 The effect of 2,6-di-(2-methylpropyl)-pyridine on the exchange rate

A sample containing 0.66 mol l^{-1} tetrapropylammonium methyltetrafluorosilicate and 1.0 mol l^{-1} in methanol showed no discernible change in the exchange rate upon the addition of 2,6-di-(2-methylpropyl)-pyridine over a concentration range of 0 to 0.52 mol l^{-1}.

5.7 The effect of pyridine on the order with respect to methanol

Figure 5.7 and table 5.5 show the effect of pyridine on the order with respect to methanol. The pyridine concentration was 1.0 mol l^{-1} and the tetrapropylammonium methyltetrafluorosilicate concentration was 0.66 mol l^{-1}. The spectra were recorded at the ambient probe temperature of 31.5°C. Within the error limits of the experiment, the order in methanol remains at 2.

5.8 The effect of temperature on the exchange rate

The effect of temperature on the pre-exchange lifetime is given in table 5.4. These values are for a solution containing 1.0 mol l^{-1} tetrapropylammonium methyltetrafluorosilicate and 1.0 mol l^{-1} in methanol. These conditions were chosen to avoid errors due to uncertainty in the orders with respect to both methanol and the fluorosilicate salt (if both $[CH_3SiF_4^-]$ and $[CH_3OH]$ both are equal to 1, $\tau^{-1} = \frac{1}{4} k$, independent of the orders). These concentrations also provided a convenient temperature range over which the exchange rate could be measured. A fit of the data to the conventional Arrhenius equation (equation 3.25) is shown in figure 5.4. The plot is quite linear to

about -30°C. Below this temperature, however, a marked curvature takes place, becoming almost a horizontal line at -50°C. A least mean squares fit developed by Deming [100] was applied to the linear portion of the plot. This resulted in a value for E_a, the activation energy, of 10.2 ± 0.3 kcal mol^{-1}. The frequency factor, A_o, was (2.1 ± 0.7) × 10^{10} s^{-1}. Figure 5.6 shows a fit to the Eyring equation (equation 3.26) for the temperature range for which the Arrhenius plot was linear. This yielded a value for the activation enthalpy, $\Delta H^{\dagger}$, of 9.6 ± 0.3 kcal mol^{-1}, and an activation entropy, $\Delta S^{\dagger}$, of -13 ± 1 cal mol^{-1} K^{-1}. The free energy of activation, $\Delta G^{\dagger}$, was found to be 13.5 ± 0.5 kcal mol^{-1} at 298 K.

The uncertainty in the temperature was estimated to be ±1°C (section 4.2), while the uncertainty in relative rate constants was estimated from the deviation between like spectra and the probable error in fitting the experimental spectra to the calculated ones. The error was generally about 10% at higher temperatures, but is higher at lower temperatures. This is due to instabilities in the spectrometer and the sensitivity of the spectrum to T_2 in this temperature region (almost the slow exchange limit). At least three spectra were recorded at each temperature, and as many as six were recorded at the lower temperatures. Figure 5.6 shows a comparison of experimental and calculated

spectra for several temperatures and τ values.

Table 5.1 The effect of methanol concentration on the pre-exchange lifetime. The sample temperature was 31.5°C, the $(CH_3SiF_4)(N(C_3H_7)_4)$ concentration was 0.66 mol l^{-1}.

$[CH_3OH]$ (mol l^{-1})†	τ^{-1} (s^{-1})†
0.233	60.3
0.317	85.6
0.449	164
0.472	191
0.497	211
0.638	403
0.670	469
0.741	518
0.905	944
0.951	854
1.11	1212
1.22	1043

† The error in the concentrations and pre-exchange lifetimes was estimated to be of the order of 10%. This value represents the average deviation from the mean of several similar samples. The average deviation of any point from the "log-log" plot was also of this magnitude.

Table 5.2 The effect of the tetrapropylammonium methyltetrafluorosilicate concentration on the pre-exchange lifetime. The methanol concentration was 1.0 mol l^{-1}.

	$[CH_3SiF_4 \quad N(C_3H_7)_4]$	τ^{-1} (s^{-1})
§	0.172	208
§	0.172	265
§	0.172	299
§	0.236	191
§	0.320	125
§	0.410	129
§	0.459	74.4
§	0.553	59.7
§	0.571	64.7
§	0.649	33.1
§	0.909	18.9
§	0.920	24.1
§	0.950	20.5
*	0.165	70.1
*	0.233	49.4
*	0.427	23.3
*	0.638	14.2
*	0.819	10.0
†	0.273	60.3
†	0.333	40.5 (cont.)

(continued from previous page)

†	0.449	31.5
†	0.549	27.1
†	0.705	16.4

§ $-17^{o}C$
* $-25^{o}C$ sample 1
† $-25^{o}C$ sample 2

Table 5.3 The effect of pyridine on the pre-exchange lifetime. The sample temperature was 31.5°C, the methanol concentration was 1.0 mol l^{-1}, and the tetrapropylammonium methyltetrafluorosilicate concentration was 0.66 mol l^{-1}.

$[C_5H_5N]$ (mol l^{-1})	τ^{-1} (s^{-1})
0.206	403
0.407	270
0.631	250
0.845	200
1.03	190
1.22	167
1.72	128
2.11	110
2.51	81.5

Table 5.4 Pre-exchange lifetimes and rate constants as a function of temperature for a solution containing 1 mol l^{-1} tetrapropylammonium methyltetrafluorosilicate and 1 mol l^{-1} methanol, in methylene chloride solution.

T (^{o}C)	T (K)*	τ^{-1} (s^{-1})	k (s^{-1} l^{x} mol^{x})†
-51	222	5 ± 2	20 ± 8
-47	226	6 ± 1	24 ± 4
-42	231	6 ± 1	24 ± 4
-37	236	6 ± 1	24 ± 4
-27	246	8 ± 1	32 ± 4
-13	260	16 ± 2	64 ± 8
-4	269	30 ± 3	120 ± 12
+17	290	115 ± 10	460 ± 40
+17	290	105 ± 10	420 ± 40
+21	294	140 ± 15	560 ± 60
+26	299	205 ± 20	820 ± 20
+32	305	285 ± 30	1140 ± 120
+40	313	440 ± 50	1760 ± 200

* Uncertainty estimated to be ± 1^{o}C.

† The exponent x is dependent on the order of the reaction with respect to the fluorosilicate. If the order is -½, then x is 1.5.

Table 5.5 The effect of methanol on the exchange rate in the presence of 1.0 mol l^{-1} pyridine. The sample temperature was 31.5°C and the tetrapropylammonium methyltetrafluorosilicate concentration was 0.66 mol l^{-1}.

$[CH_3OH]$ (mol l^{-1})	τ^{-1} (s^{-1})
0.84	83.1
1.65	330
2.51	639

Figure 5.1 A plot showing the effect of methanol concentration on the exchange rate. From the slope of the graph the kinetic order with respect to methanol may be determined. The estimated error limits are shown for one point.

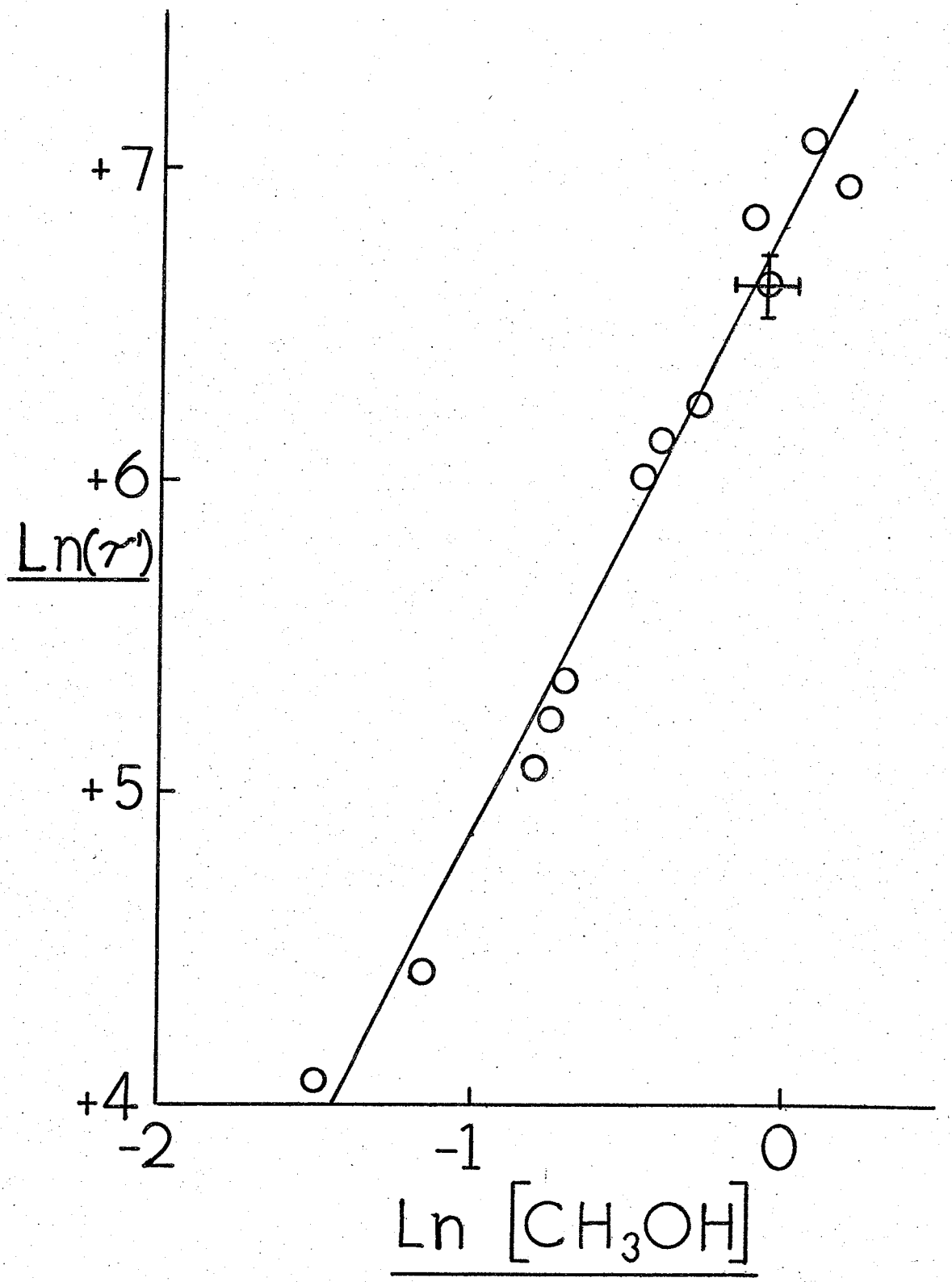
+7
+6
+5
+4
Ln(τ')
-2
-1
0
Ln [CH3OH]

Figure 5.2 A graph showing the effect of tetra-propylammonium methyltetrafluorosilicate concentration on the exchange rate. Note that the effect is a reduction of exchange rate as the concentration is increased. The kinetic order may me determined from the slope of the lines as described in the text. Typical error limits are shown for one point.

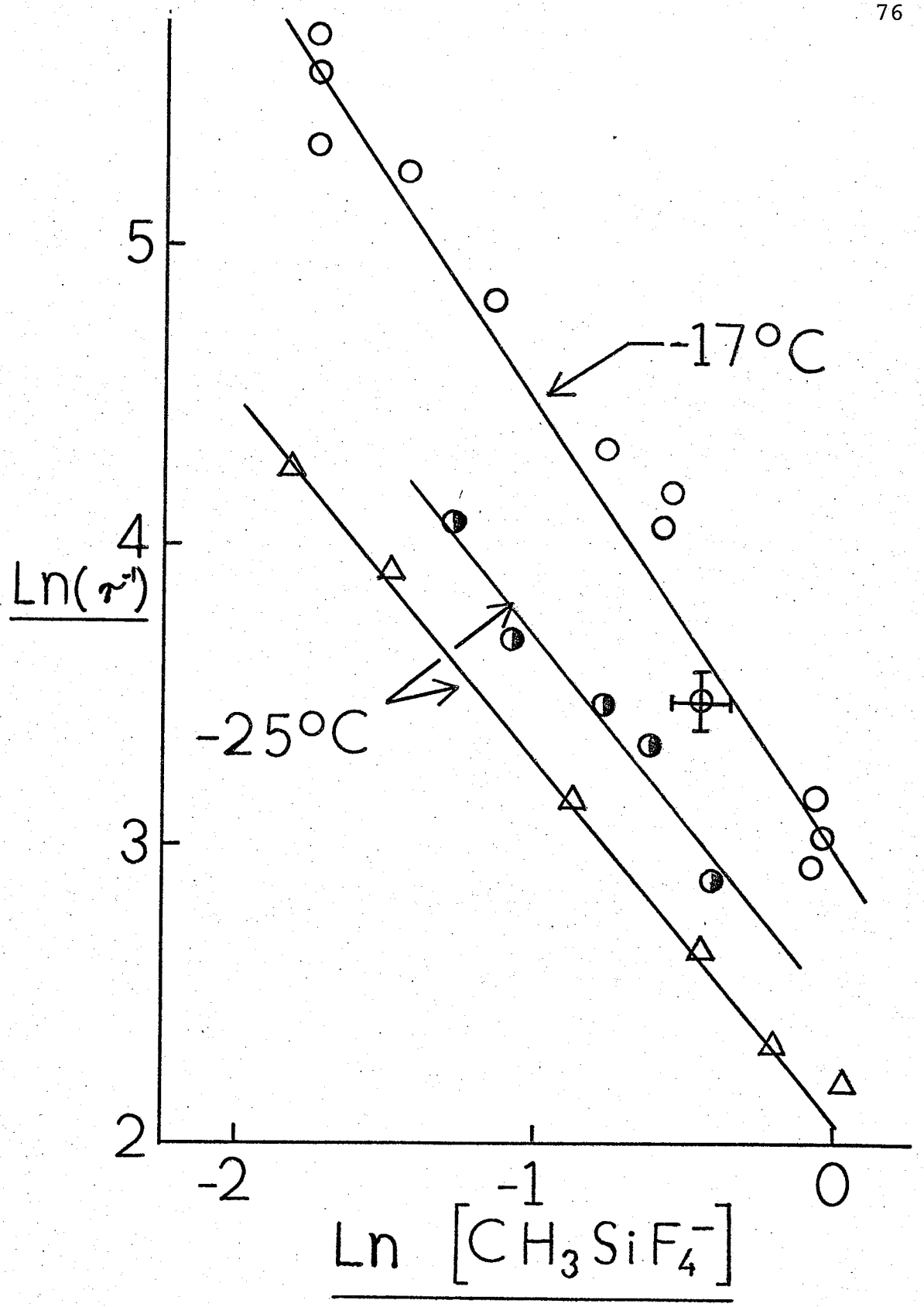
5
4
3
2
Ln(τ⁻¹)
-17°C
-25°C
-2
-1
0
Ln [CH3SiF4⁻]

Figure 5.3 The effect of pyridine on the exchange rate. Typical error limits are shown for one point.

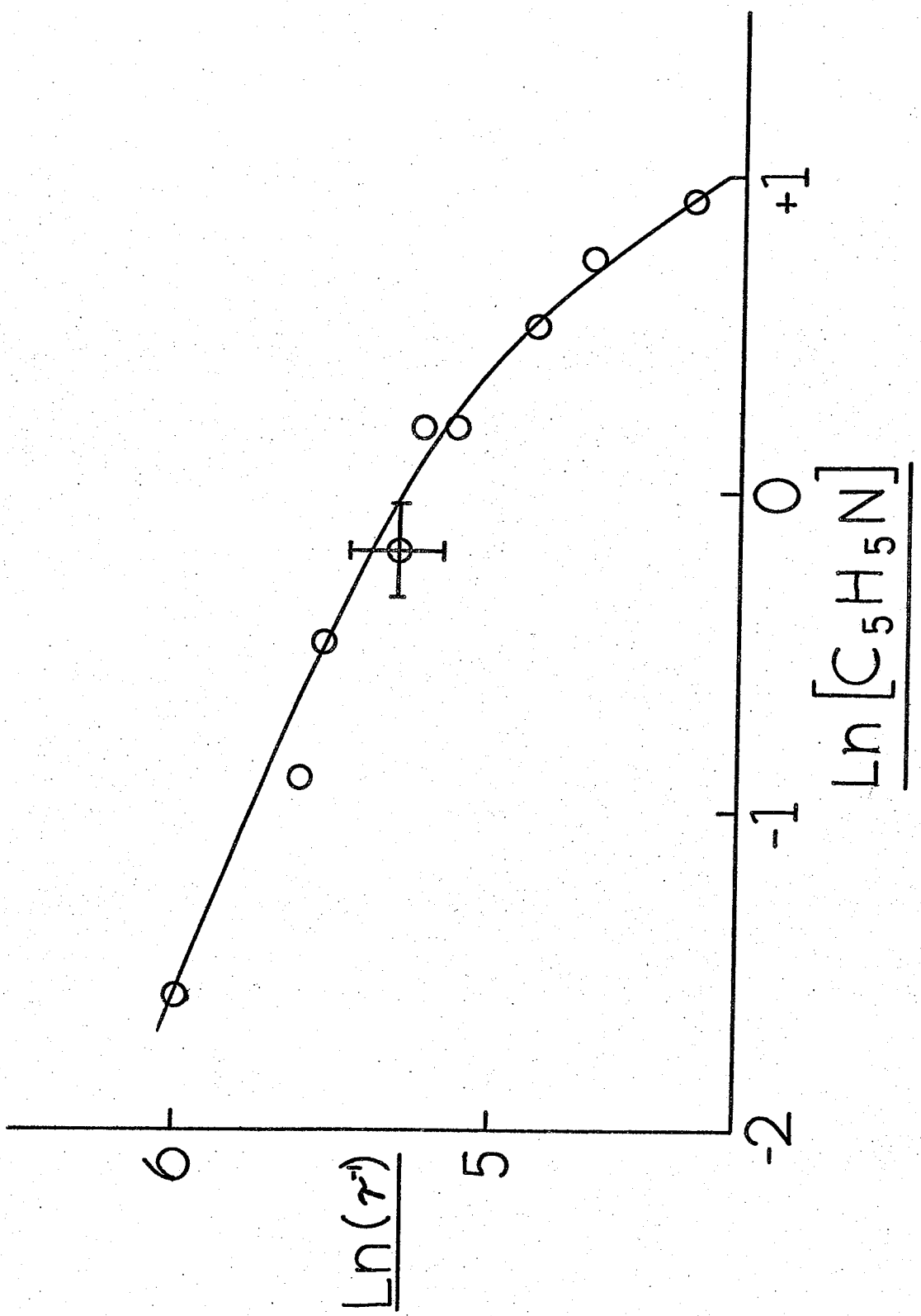
6
5
Ln(τ̄)
-2
-1
0
+1
Ln [C5H5N]

Figure 5.4 An "Arrhenius" plot for the methanol catalyzed fluorine exchange in tetrapropylammonium methyltetrafluorosilicate. Possible reasons for the curvature are discussed in chapter 6 and in Appendix C. The activation parameters are given in the text.

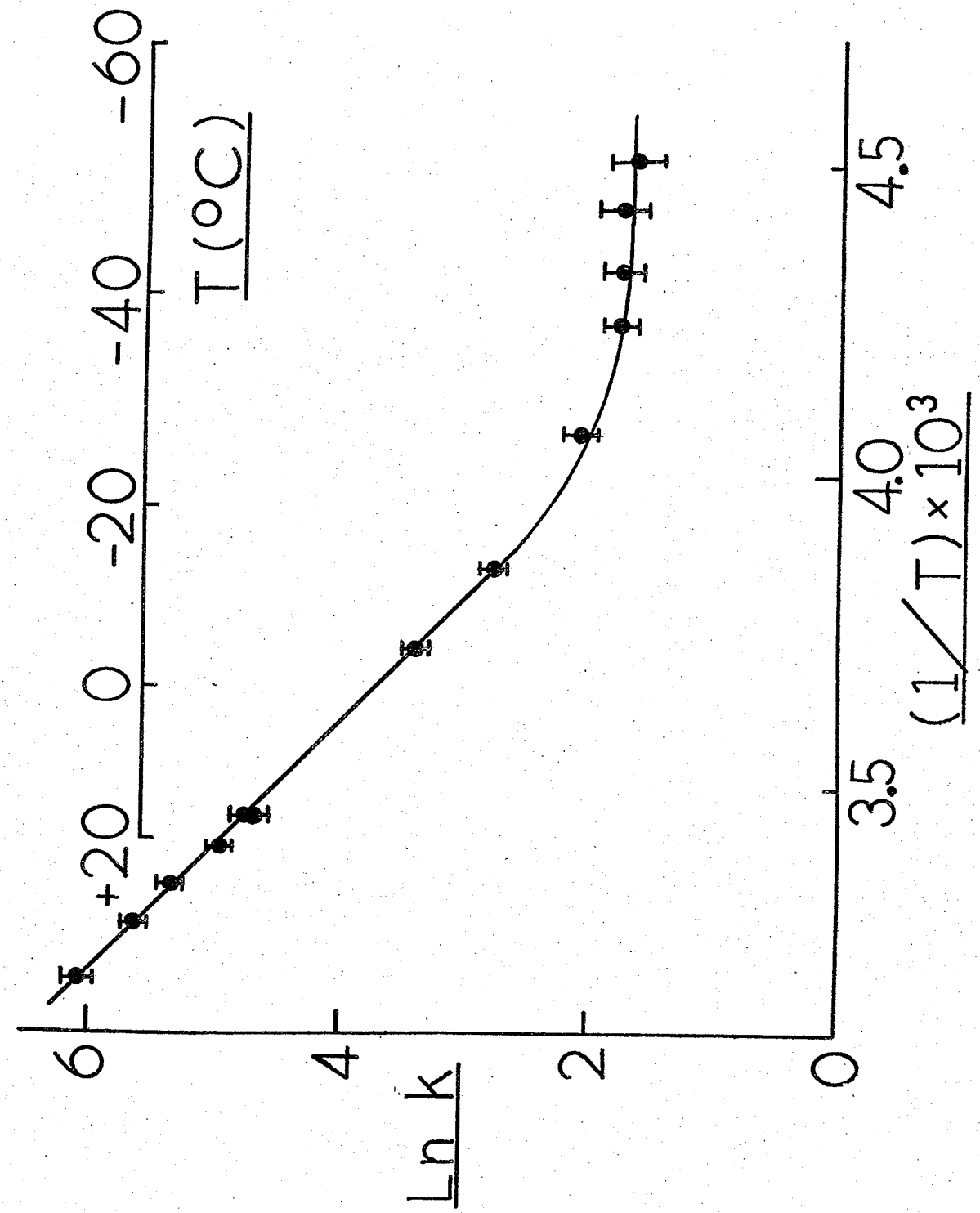
T(°C)
+20
0
-20
-40
-60
Ln k
6
4
2
0
3.5
4.0
4.5
(1/T) x 10³

Figure 5.5 An "Eyring" plot for the methanol catalyzed fluorine exchange in tetrapropylammonium methyltetrafluorosilicate. Only the region over which the "Arrhenius" plot is linear is shown.

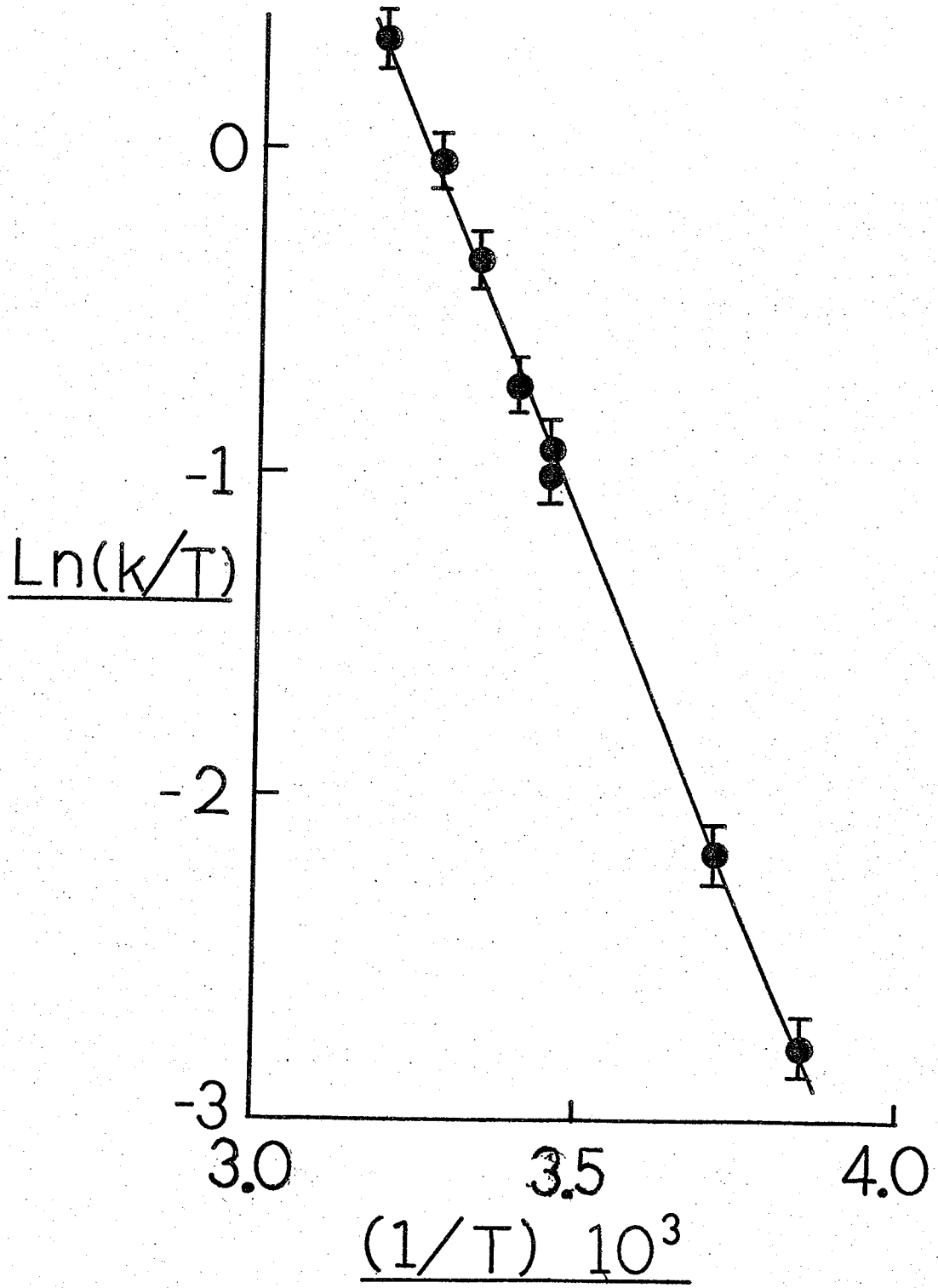
0
-1
-2
-3
Ln(k/T)
3.0
3.5
4.0
(1/T) 10³

Figure 5.6 A comparison of experimental and calculated spectra for three different temperatures. The experimental spectra are on the left, and the calculated spectra are on the right.

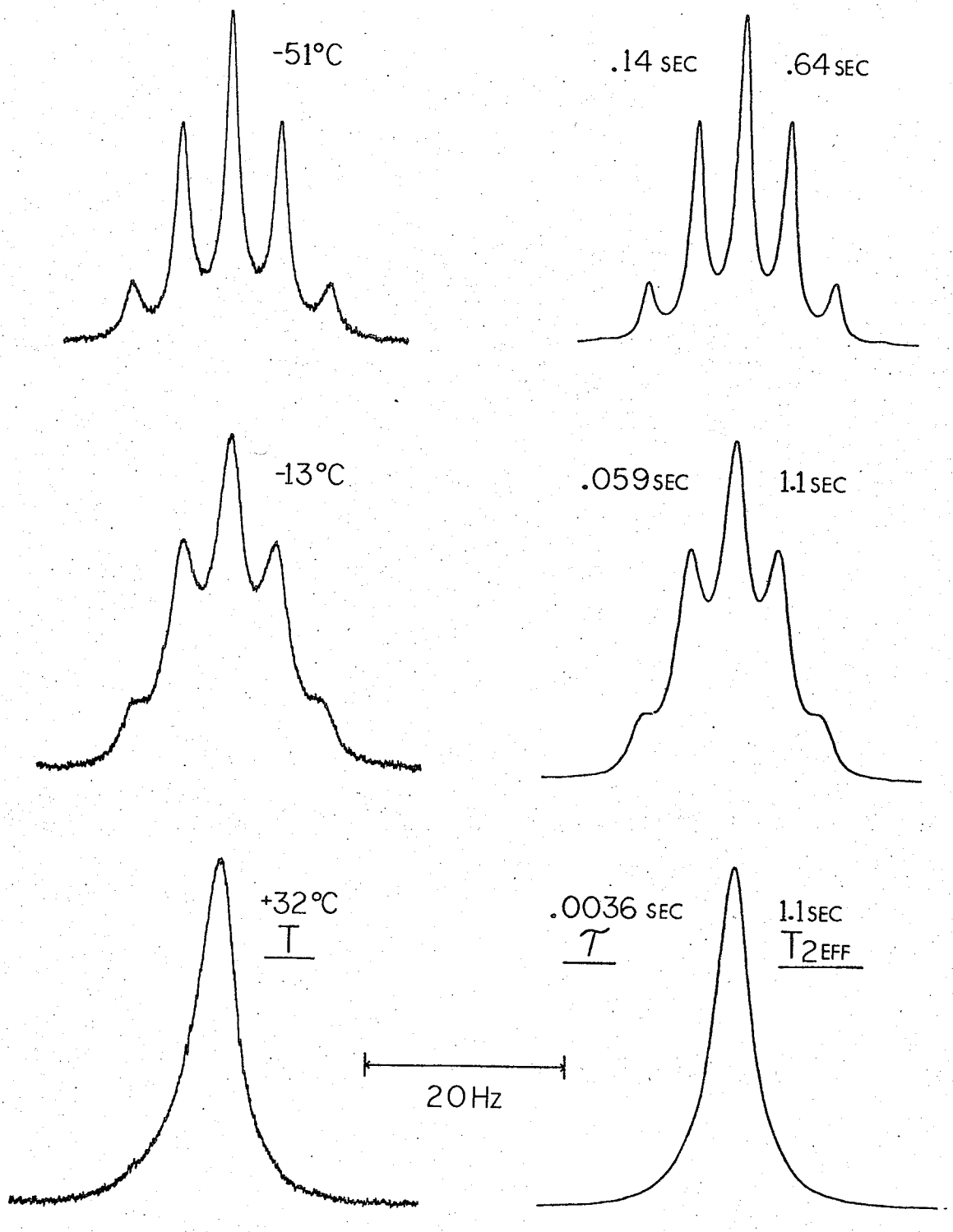
-51°C
.14 SEC
.64 SEC
-13°C
.059 SEC
1.1 SEC
+32°C
T
.0036 SEC
τ
1.1 SEC
T2 EFF
20 Hz

Figure 5.7 The effect of methanol on the exchange rate in the presence of 1.0 mol l^{-1} pyridine. The tetrapropylammonium methyltetrafluorosilicate concentration was 0.66 mol l^{-1}.

The slope of the line is 2.0 ± 0.2.

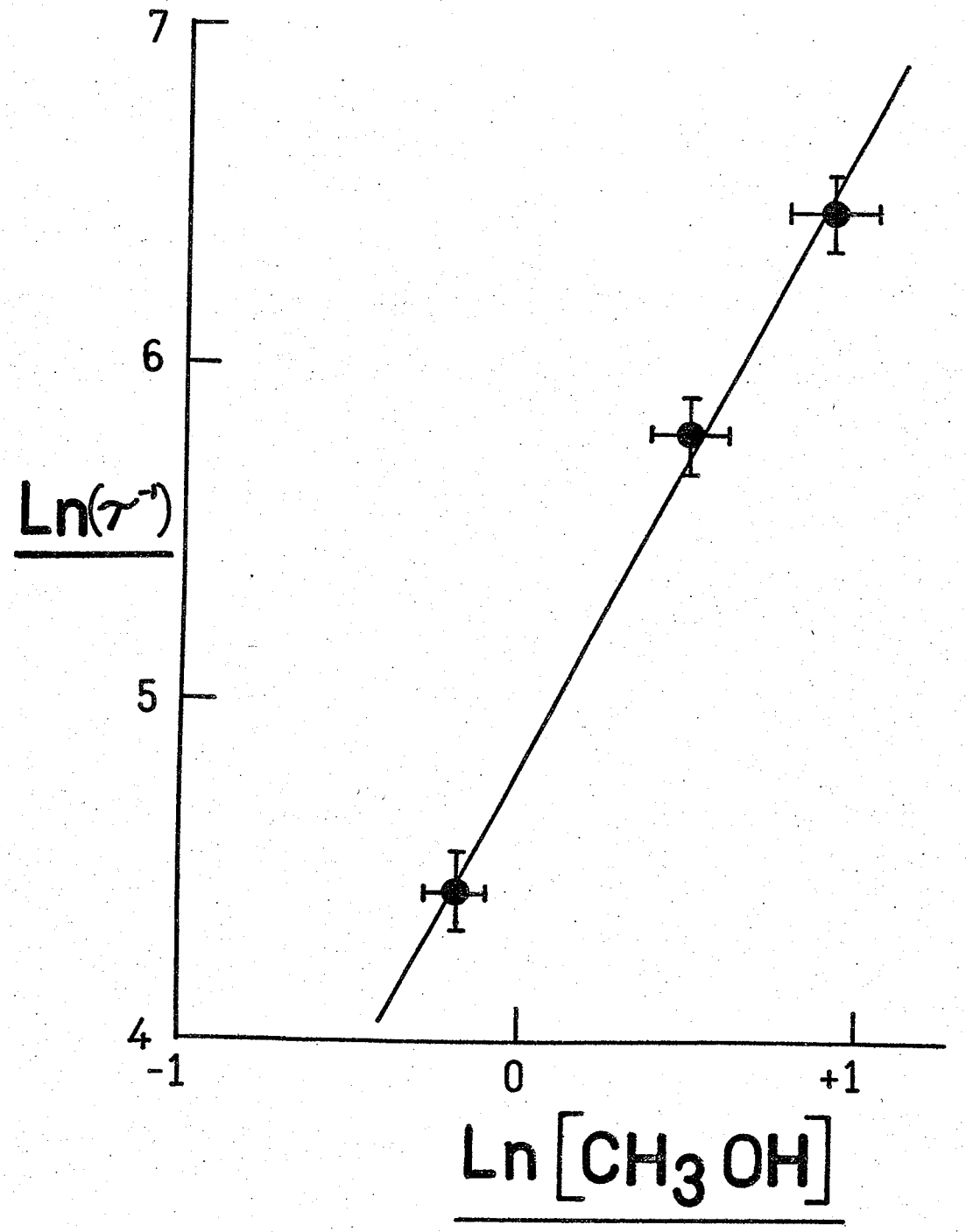
7
6
5
4
Ln(τ⁻¹)
-1
0
+1
Ln [CH3 OH]

CHAPTER 6 DISCUSSION

With the kinetic data available, it is now possible to propose mechanisms that are consistent with the experimental observations.

The first step in any possible mechanism is probably the dissociation of the ion-pair into the separate ions.

$$\underset{\underline{A}}{\left[CH_3SiF_4 \quad N(C_3H_7)_4\right]} \rightleftharpoons \underset{\underline{B}}{CH_3SiF_4^-} + \underset{\underline{C}}{{}^+N(C_3H_7)_4}$$

(step 1)

It is reasonable to assume that it is only the free $CH_3SiF_4^-$ ion that is involved in the exchange process. It is also reasonable to assume that the equilibrium described by step 1 is well to the left in a non-polar solvent such as methylene chloride. These assumptions are supported by analogy to the dnmr studies on $(C_4H_9)_4N$ PF_6,[58] and by molecular weight measurements. The molecular weight expected for the ion-pair is 305 g mol^{-1}, while for the individual ions the apparent molecular weight would be one half of this value. The experimental value was found to be 330 ± 20 g mol^{-1}. The slight difference between the experimental and formula weights may be due to a tendency to higher aggregation or, more probably, a

deviation from Raoult's law. Extensive ion-pairing has been observed for a number of related compounds in non-polar solvents.[58,101] If extensive ion-pair formation occurs, then:

$$K_1 = \frac{[B]\ [C]}{[A]} \qquad (6.1)$$

$$[B] = K_1^{\frac{1}{2}}\ [A]^{\frac{1}{2}} \qquad (6.2)$$

Before proposing any new mechanisms, an examination of Klanberg's and Muetterties' mechanisms is in order. Their first mechanism was a bimolecular exchange involving the formation of fluorine bridged dimers, thus:

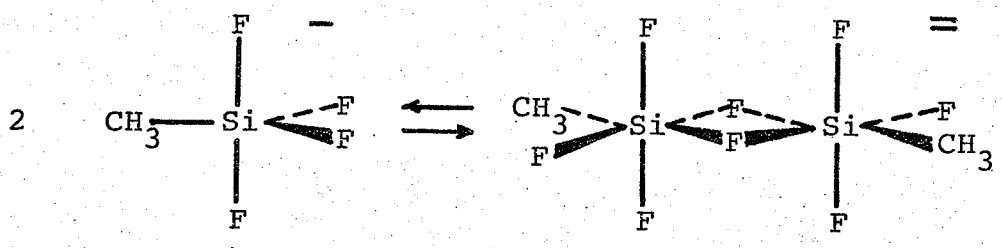

This step would have the following rate law:

$$(\text{rate}) = k\ [B]^2 \qquad (6.3)$$

(rate) refers to the macroscopic fluorine exchange rate on a d(concentration)/dt basis.

Combining equations 6.2 and 6.3 results in:

$$(\text{rate}) = k K_1 [A]$$

$$\tau^{-1} = \frac{1}{4} k K_1 [A]^0 \qquad (6.4)$$

The inverse of the pre-exchange lifetime would be independent of the added salt concentration. This is not what is found experimentally. Indeed, the inverse of the pre-exchange lifetime is inversely proportional to some non-integral power of the salt concentration. This strongly suggests that a fluorine bridged dimer is not the predominent mechanism for fluorine exchange.

The other proposed mechanism (the one that Klanberg and Muetterties preferred for the $CH_3SiF_4^-$ ion) was an ionization process.

$$CH_3SiF_4^- \rightleftharpoons CH_3SiF_3 + F^-$$

In this case, the exchange would be first order in $CH_3SiF_4^-$.

$$(\text{rate}) = k [B]$$

$$(\text{rate}) = k K_1^{\frac{1}{2}} [A]^{\frac{1}{2}}$$

$$\tau^{-1} = \frac{1}{4} k K_1^{\frac{1}{2}} [A]^{-\frac{1}{2}}$$

The observed order, on a lifetime basis, would be -1/2, similar to the case of PF_6^-.[58] Since the observed order is actually -1.2 to -1.5, this mechanism also does not adequately explain the kinetics. More importantly, neither of these mechanisms explain the need for two molecules of methanol in the mechanism. In the absence of methanol, a carefully purified sample shows no exchange on the nmr time scale. This indicates that if any exchange occurs via either of these two mechanisms, it must be too slow to observe with a dnmr technique.

Having eliminated the previous mechanisms as inconsistent with the experimental findings, it is necessary to propose mechanisms that <u>are</u> consistent with the kinetics, and are also consistent with the known chemistry of these compounds.

<u>Scheme 1</u>

One possible explanation for the second order dependency on methanol involves the establishment of a pre-equilibrium of $CH_3SiF_4^-$ and methanol in a Lewis-acid Lewis-base adduct.

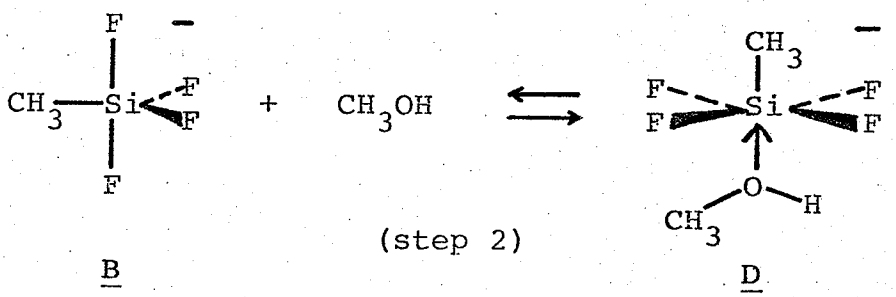

B (step 2) D

It is reasonable to assume that this equilibrium is well to the left, since the $SiF_5{:}NH_3^-$ adduct has been found to lie essentially to the left in CH_2Cl_2 solution.[2,3]† If this is the case, the concentration of the complex will be:

$$[D] = K_2 [B] [CH_3OH] \qquad (6.5)$$

Combining equations 6.1 and 6.5 gives:

$$[D] = K_2 K_1^{\frac{1}{2}} [A]^{\frac{1}{2}} [CH_3OH]$$

Now, if the proton can be abstracted by a second molecule of methanol.

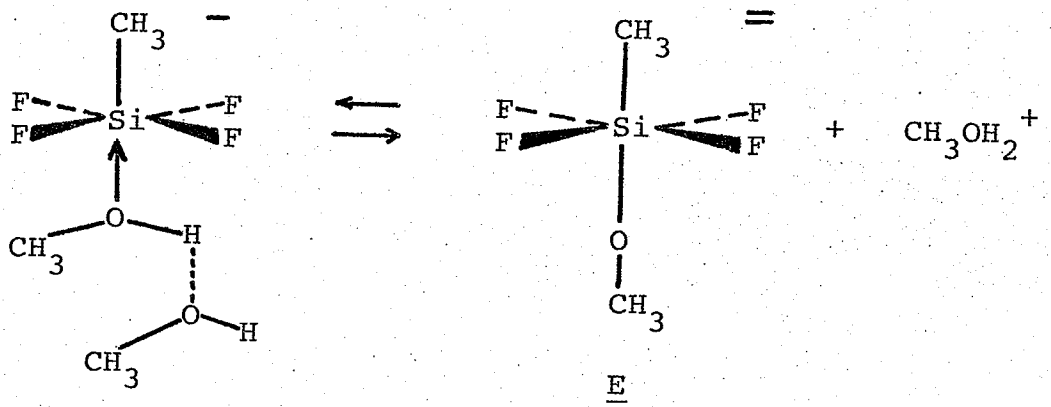

(step 3)

† Adducts of SiF_5^- are well known.[2,3,102-104]

Then:

$$[E] = K_3 [D] [CH_3OH]$$

$$[E] = K_3 K_2 K_1^{\frac{1}{2}} [A]^{\frac{1}{2}} [CH_3OH]^2 \qquad (6.7)$$

If the six coordinate intermediate, E, is unstable enough, it may return to five coordination by loss of a fluorine.†

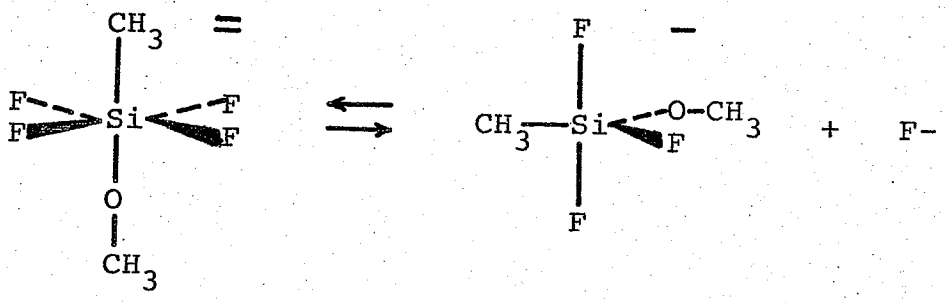

E (step 4) F

This would be a first order process in E with a first order rate constant, k_1.

$$(\text{rate}) = k_1 [E]$$

$$(\text{rate}) = k_1 K_3 K_2 K_1^{\frac{1}{2}} [A]^{\frac{1}{2}} [CH_3OH]^2$$

$$\tau^{-1} = \frac{1}{4} k_1 K_3 K_2 K_1^{\frac{1}{2}} [A]^{-\frac{1}{2}} [CH_3OH]^2 \qquad (6.8)$$

---

† This is entirely possible, since no six coordinate silicon fluorides (except for $SiF_6^=$ and $SiF_5{:}B^-$) have been characterized by nmr. Excess fluoride in the production of $CH_3SiF_4^-$ does not result in a stable $CH_3SiF_5^=$.(1,85)

This expression for the inverse of the pre-exchange lifetime is proportional to the second power of the methanol concentration, and inversely proportional to the square root of the tetrapropylammonium methyltetrafluorosilicate concentration. This mechanism still does not reproduce the -1.2 to -1.5 order found experimentally.

It is possible that one of the products of a later step in the reaction inhibits some earlier step. One possibility might be for the fluoride formed in step 4 to complex with the $CH_3SiF_4^-$ ion.

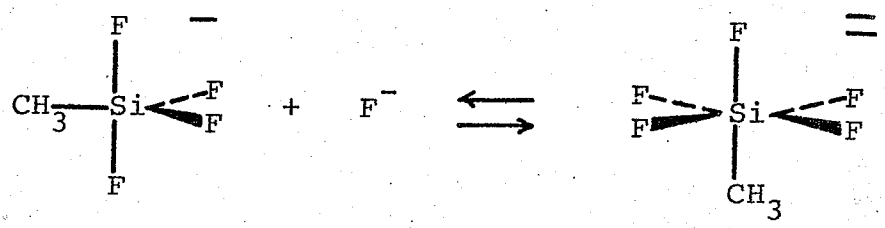

If the rate of this exchange was slow compared to the exchange in step 4, it could inhibit the reaction by "tying up" F^- and $CH_3SiF_4^-$. This would even be more reasonable if $CH_3SiF_4^-$ was a much better fluoride acceptor than $CH_3(OCH_3)SiF_3^-$. No studies of the acceptor properties of these ions have been undertaken, but since fluorine is a better electron acceptor than a methoxy group, this would be expected.

Scheme 2

Another possibility for the exchange mechanism might be:

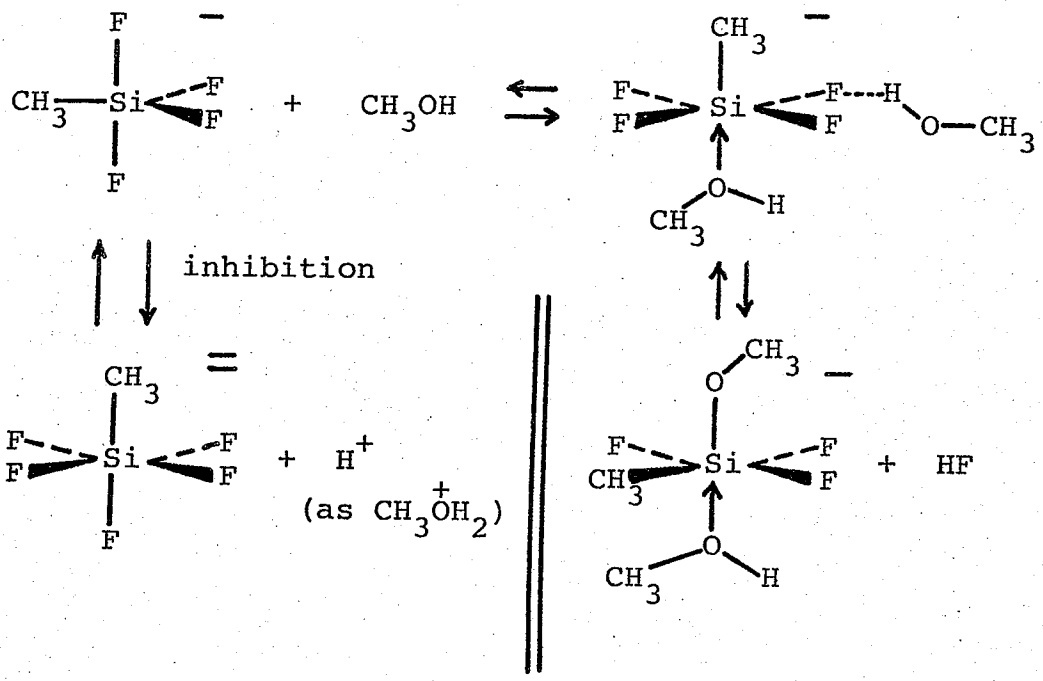

This would also explain the kinetic results.

Scheme 3

Another possibility might be:

$$2\ CH_3OH \rightleftharpoons CH_3OH_2^+ + CH_3O^-$$

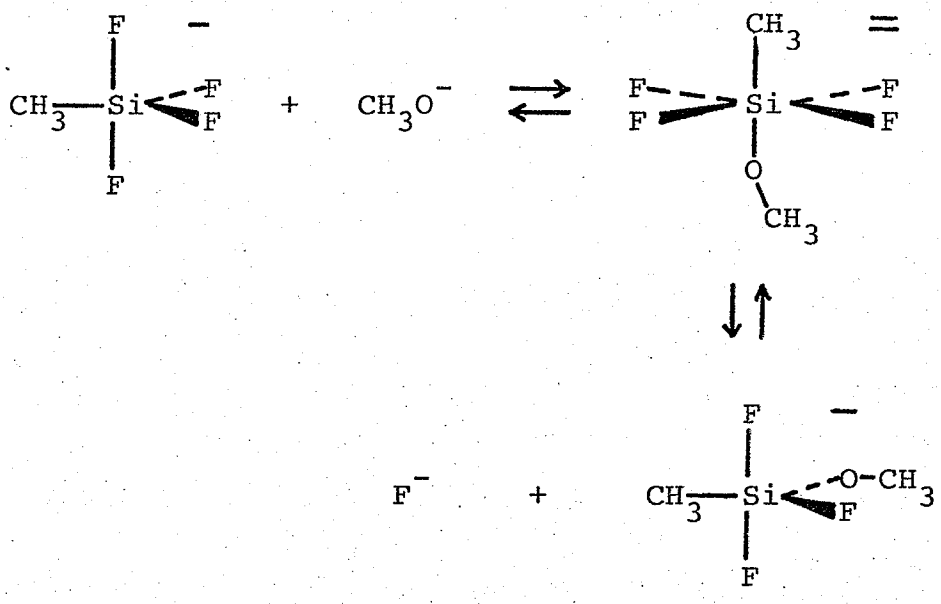

which could also be inhibited by fluoride at the first stage. This mechanism is not as attractive as the others, since the equilibrium constant for the first step would be unfavourable, especially in methylene chloride solution.

Another possible explanation for the second order dependence on methanol is a change in the bulk properties of the solvent due to the relatively high concentrations of methanol employed.[105] One way for this to occur would be an increase in the $CH_3SiF_4^-$ concentration due to a change in the equilibrium constant K_1. This would be entirely possible, since methanol would be expected to solvate the ions better than methylene chloride. For this to result in second order kinetics over the ten-fold concentration range studied would be purely fortuitous.

In order to test the hypothesis that the exchange could be inhibited by a Lewis-base at the first step, it

was decided to study the effect of pyridine on the exchange rate. A decrease in the rate is noted, and this may be due to the following situation:

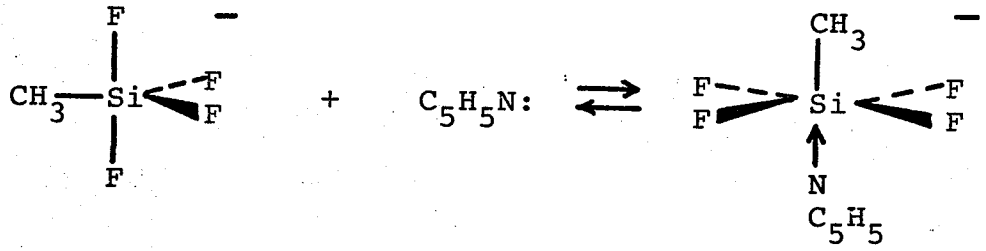

Since there are at least several equilibria in competition with this one, it would be impossible to quantify this effect without detailed knowledge of the steps involved. Nevertheless, it is clear that reducing the concentration of the $CH_3SiF_4^-$ ion in this manner should reduce the exchange rate (if the previously described mechanisms have any validity).

It is also possible that pyridine could inhibit the exchange by complexing with any hydrogen fluoride involved in the reaction. To test this hypothesis, 2,6-di-(2-methylpropyl)-pyridine was added to an exchanging sample. This material should be capable of complexing with hydrogen fluoride,† but it should be too hindered at the nitrogen

---

† The K_a value for this base is not known.

to form an adduct with the fluorosilicate anion. The rate is found to be neither accelerated nor hindered by the introduction of this base; therefore, it may be concluded that hydrogen fluoride is probably not involved in the reaction mechanism.

An ideal test of the hypothesis that the exchange is inhibited by fluoride ion would be the direct introduction of a fluoride salt into the system. This proved impossible, however, since no fluoride salt soluble enough in methylene chloride and at the same time pure enough for these studies could be found. Commercial tetraalkylammonium fluorides generally are available only as the hydrates, and have also been found to contain up to 10% chloride.[1] Tetrapropylammonium fluoride prepared by the author always contained traces of water and the bifluoride, as detected by infrared spectroscopy. It should be noted that these materials are very hygroscopic, and since water is probably a very efficient catalyst of fluorine exchange, the results obtained upon the addition of these fluorides would probably be unreliable.

It is important to realize that activation parameters determined by the conventional Arrhenius and Eyring methods represent thermodynamic properties of the transition state (or activated complex) only when the rate being studied is that of an elementary process.[106,107] Since the

"rate constant" determined by the dnmr method can be a collection of rate constants and equilibrium constants, the results obtained are a composite of terms. For an example of how a pre-equilibrium can effect an activation energy the reader is directed to Appendix C. Without detailed knowledge of the equilibria involved the activation parameters provide an empirical method for describing the effects of temperature on the exchange rate.

One interesting feature of this system is the fact that the overall activation entropy was found to be negative (-13 ± 1 cal mol^{-1} K^{-1}). This indicates that at least one of the steps in the exchange process must have a negative entropy. This is entirely consistent with a mechanism involving the formation of a complex or complexes. Complex formation is an ordering of the system, a counter-entropic process. Dissociative processes, on the other hand, generally have positive entropies of activation and positive equilibrium entropies. This negative entropy tends to support the hypothesis that expansion from five to six coordination takes place at some point in the exchange process. Expansion to five and six coordination has been postulated as the mechanism for the racemisation of chlorosilanes [108-111] and in the base catalyzed hydrolysis of trimethylfluorosilane.[2,6] Six coordination has also been postulated in the racemisation of triorganotin halides.[112] These mechanisms are all supported by the kinetics.

Another interesting feature of the Arrhenius plot is the rather unusual change in slope at low temperatures. This may also be a consequence of a multi-step reaction, but another more probable explanation is given in Appendix B. Reviews on the effects of equilibria on Arrhenius plots have been given by Hulett and others.[119-121]

APPENDIX A SIMPLIFIED FLOW CHART OF PROGRAM "EXCHSYS"

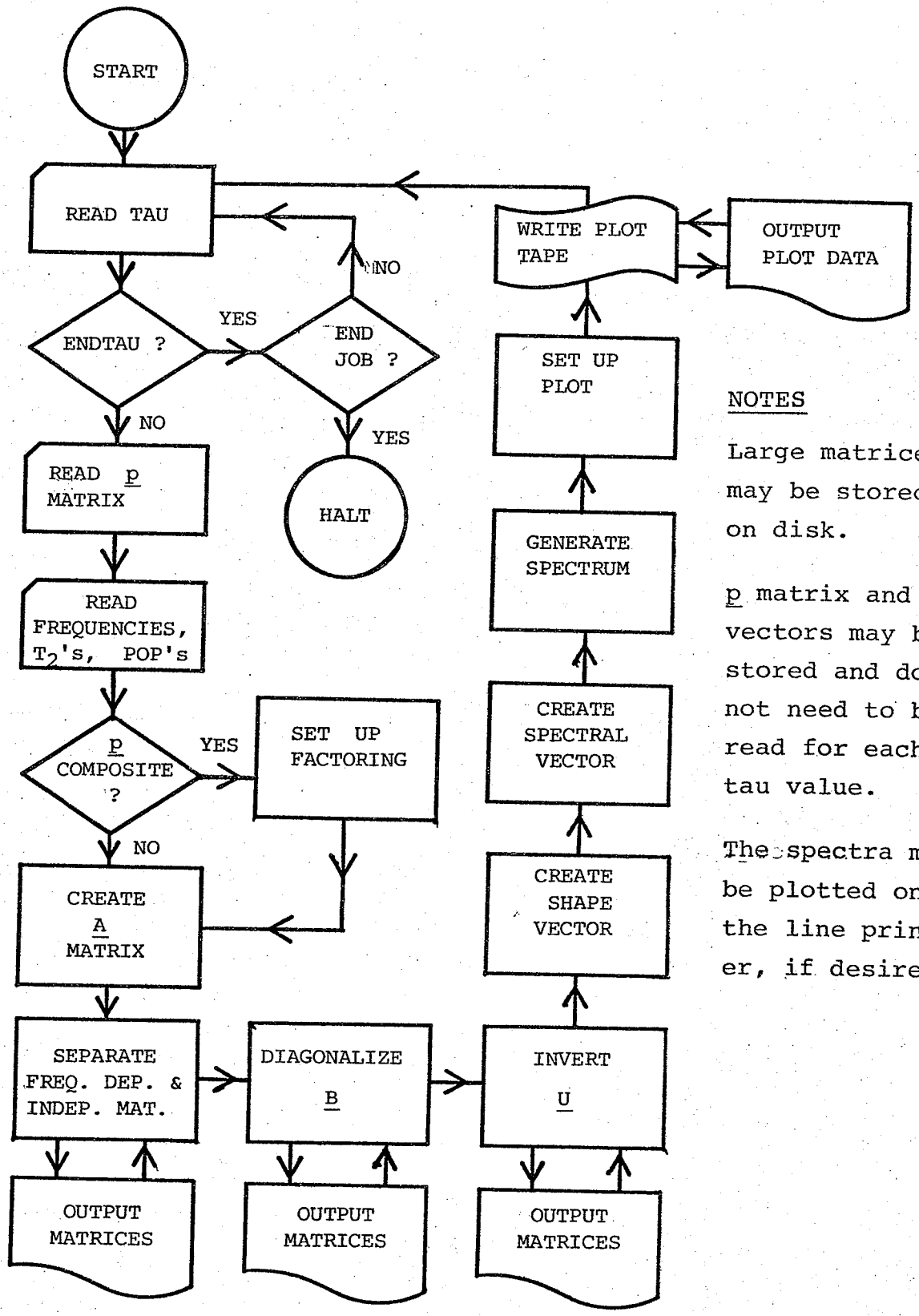

NOTES

Large matrices may be stored on disk.

p matrix and vectors may be stored and do not need to be read for each tau value.

The spectra may be plotted on the line printer, if desired.

APPENDIX B THE EFFECTS OF FLUORINE SPIN LATTICE RELAXATION ON THE PROTON LINESHAPE

In chapter 6 it was pointed out that a shift in an equilibrium may be responsible for the abrupt change in slope of the Arrhenius plot. Another possibility is that an exchange in fluorine spin states might occur via a fluorine T_1 process, since a change in spin state of one of the four fluorines is equivalent to an intermolecular exchange of the fluorine for one of the opposite spin.

It is known that for an absorption mode Lorentzian line, a plot of

$$\frac{\lim_{B_1 \to 0} \frac{A}{B_1}}{\frac{A}{B_1}} \qquad \text{(B1)}$$

as a function of B_1^2 will have a slope of $\gamma^2 T_1 T_2$, where A is the amplitude of the resonance absorption.[113] γ, T_1, T_2 and B_1 are defined in chapter 3. Since γ is known,[114] and B_1 may be easily measured,[98] and T_2 may be determined from the linewidth at half height (provided $T_2 << T_1$) T_1 may be obtained. For a 0.66 mol l^{-1} solution of tetrapropylammonium methyltetrafluorosilicate in a 1.0 mol l^{-1} CH_2Cl_2 solution of methanol, T_1 was 1.7 s and T_2 was 31.8 ms.

These values were obtained at the ambient probe temperature of 30 ± 1 ^{o}C, the only temperature available at the time.

In most instances T_1 values decrease with a decrease in temperature. For this reason, any possible effects of relaxation on the apparent exchange rate will be more pronounced at lower temperatures. The temperature dependence of relaxation rates may be determined with the following equation:

$$R_1 = R_o \exp(E_a/RT) \qquad (B2)$$

where $R_1 = T_1^{-1}$ and E_a is an empirical "activation energy" for the relaxation process. Assuming a "typical" activation energy of 3 kcal mol^{-1} the value of R_1 at -50^{o}C was estimated to be 2.6 s^{-1}, which is equivalent to a fluorine exchange rate of 5.2 s^{-1} (since one-half of all fluorine exchanges result in no change in the magnetic state of the ion). This compares quite favourably with the experimental value of 6 ± 1 s^{-1} for this temperature. This agreement may be purely fortuitous, of course, but the calculation serves to illustrate the manner in which a relaxation process could become comparable to the exchange process at low temperatures. The "expected" exchange rate, based on the Arrhenius law, would be less than 1 s^{-1} at this temperature.

It is interesting to speculate on what the cause of this relaxation might be. The predominent mechanism is

likely to be dipole-dipole relaxation,[115] in which case the relaxation rate will be given by:[116]

$$R_1 = \frac{2\gamma^4 \hbar^2 I(I+1)}{r^6} \tau_c \qquad \text{(B3)}$$

where $\hbar$ is Planck's constant divided by 2π, r is the inter-dipole distance, I is the spin quantum number of the nucleus and τ_c is the rotational correlation time. Since X-ray crystallographic data for the $CH_3SiF_4^-$ ion were not available, it was necessary to use the bond lengths of SiF_5^-, which the most reliable work gives as 1.7×10^{-8} cm.[117] Each fluorine is then at a distance of 2.4×10^{-8} cm from two others. The distance to any other nuclei is 3×10^{-8} cm at the nearest. Since the rate is proportional to r^{-6}, the relaxation from these other nuclei may be ignored. The following diagram provides a clarification of the situation.

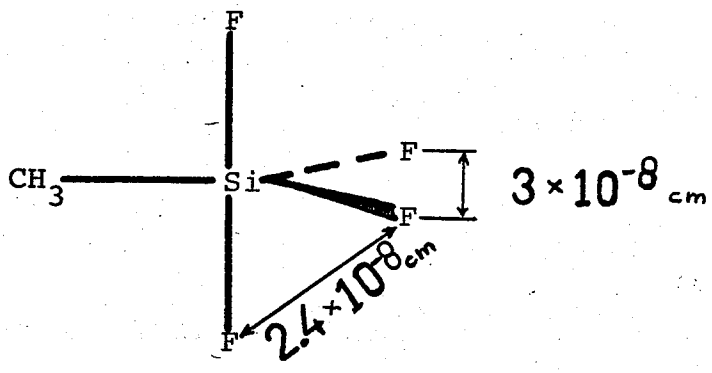

Using the 2.4×10^{-8} cm value, and considering that each

fluorine is relaxed by two others, results in:

$$R_1 = 6.92 \times 10^9 \quad \tau_c$$

τ_c is unknown but may be assumed to be about 10^{-10} to 10^{-11} s for a species of this molecular weight (305) at room temperature. This assumes, of course, that the ion spends most of the time bound in the ion-pair. A correlation time of these magnitudes will result in a T_1 value of between 1.4 and 14 s. This may be compared to the experimental value of 1.7 s. These calculations are admittedly very crude and many possible relaxation mechanisms have not been included. They do, however, show that dipole-dipole relaxation must be an important term in the total relaxation rate of the $CH_3SiF_4^-$ ion.

APPENDIX C THE EFFECT OF A RAPID PRE-EQUILIBRIUM ON AN OBSERVED ACTIVATION ENERGY

Consider the following reaction sequence

$$A + B \rightleftharpoons C$$

$$C \longrightarrow D$$

in which the rate of formation of D is measured.

$$\frac{d[D]}{dt} = k[C] \qquad (C1)$$

But

$$[C] = K_{eq}[A][B] \qquad (C2)$$

Combining C1 and C2 results in:

$$\frac{d[D]}{dt} = k K_{eq}[A][B]$$

This reaction will be observed to be first order in A and first order in B with an observed rate constant, k_{obs}, which is the product of the first step equilibrium constant and the second step rate constant.

In an Arrhenius treatment, the logarithm of k_{obs}

would be plotted as a function of T^{-1} from which an "activation energy" could be determined. Since k_{obs} is a composite of two terms, the "activation energy" will be a composite of two terms.

$$k = A \exp(-E_a/RT) \tag{C3}$$

$$K_{eq} \tilde{=} B \exp(-\Delta H/RT) \tag{C4}$$

$$k_{obs} = A \exp(-Ea/RT) \cdot B \exp(-\Delta H/RT) \tag{C5}$$

$$\ln k_{obs} = \ln A + \ln B - \frac{E_a}{RT} - \frac{\Delta H}{RT} \tag{C6}$$

Therefore, a plot of $\ln k_{obs}$ as a function of T^{-1} will give an apparent "activation energy" of $E_a + \Delta H$. In other words, the "activation energy" will be the sum of the activation energy for the second step and the enthalpy for the equilibrium. The pre-exponential factor will be the sum of the sum of the frequency factor in equation C3 (A) and the constant of integration in equation C4 (B).

REFERENCES

1. F. Klanberg and E. Muetterties, Inorganic Chemistry, 7, 155 (1968).

2. J. A. Gibson, Ph.D. Thesis, University of Manitoba, (1973).

3. J. A. Gibson, D. G. Ibbott and A. F. Janzen, Can. J. Chem., 51, 3203 (1973).

4. A. F. Janzen, J. A. Gibson and D. G. Ibbott, Inorganic Chemistry, 11, 2853 (1972).

5. D. G. Ibbott and A. F. Janzen, Can. J. Chem., 50, 2428 (1972).

6. J. A. Gibson and A. F. Janzen, Can. J. Chem., 50, 3087 (1972).

7. R. Luchenbach, Dynamic Stereochemistry of Pentacoordinate Phosphorus and Related Elements, Georg Thieme, Stuttgart (1973).

8. C. Eaborn, Organosilicon Compounds, Butterworths, London (1960).

9. L. H. Sommer, Stereochemistry, Mechanism and Silicon, McGraw-Hill, New York (1965).

10. F. Bloch, Phys. Rev., 70, 460 (1946).

11. H. S. Gutowsky, D. W. McCall and C. P. Slichter, J. Chem. Phys., 21, 279 (1953).

12. H. S. Gutowsky and A. Saika, J. Chem. Phys., 21, 1688 (1953).

13. H. S. Gutowsky and C. H. Holm, J. Chem. Phys., 25, 1228 (1956).

14. H. M. McConnell, J. Chem. Phys., 26, 430 (1958).

15. L. W. Reeves and K. N. Shaw., Can. J. Chem., 48, 3641 (1970).

16. E. A. Allan, M. G. Hogben, L. W. Reeves and K. N. Shaw, Pure and Applied Chemistry, 32, 9 (1972).

17. L. W. Reeves and K. N. Shaw, Can. J. Chem., 49, 3671 (1971).

18. L. W. Reeves and K. N. Shaw, Can. J. Chem., 49, 3683 (1971).

19. S. O. Chan and L. W. Reeves, J. Am. Chem. Soc., 95, 673 (1973).

20. R. F. Hobson and L. W. Reeves, J. Phys. Chem., 77, 419 (1973).

21. C. S. Johnson, Adv. Mag. Res., 1, 33 (1965).

22. G. Binsch, Topics in Stereochemistry, 3, 97 (1968).

23. I. O. Sutherland, Annual Reports on N.M.R. Spectroscopy, 4, 71 (1971).

24. J. I. Kaplan, J. Chem. Phys., 28, 278 (1958).

25. J. I. Kaplan, J. Chem. Phys., 29, 462 (1958).

26. S. Alexander, J. Chem. Phys., 37, 967 (1962).

27. S. Alexander, J. Chem. Phys., 37, 974 (1962).

28. S. Alexander, J. Chem. Phys., 38, 1787 (1963).

29. S. Alexander, J. Chem. Phys., 40, 2741 (1964).

30. R. A. Sack, Mol. Phys., 1, 163 (1958).

31. R. Kubo and K. Tomita, J. Phys. Soc. Japan, 9, 888 (1954).

32. R. Kubo, J. Phys. Soc. Japan, 9, 935 (1954).

33. R. Kubo, Nuovo Cheminto. Suppl., 6, 1063 (1957).

34. P. W. Anderson, J. Phys. Soc. Japan, 9, 316 (1954).

35. L. H. Piette and W. A. Anderson, J. Chem. Phys., 30, 899 (1959).

36. J. T. Arnold, Phys. Rev., 102, 136 (1956).

37. G. M. Whitesides, Ph.D. Thesis, California Institute of Technology (1964).

38. J. P. Jesson and P. Meakin, Accounts of Chemical Research, 6, 269 (1973).

39. G. Binsch, J. Am. Chem. Soc., 91, 1304 (1969).

40. D. A. Kleier and G. Binsch, J. Mag. Res., 3 146 (1970).

41. P. Meakin, E. L. Muetterties and J. P. Jesson, J. Am. Chem. Soc., 95, 75 (1973).

42. G. Binsch and D. A. Kleier, "The Computation of Complex Exchange Broadened NMR Spectra," Program 140, Quantum Chemistry Program Exchange (1969).

43. D. A. Kleier and G. Binsch, "A Computer Program for the Calculation of Complex Exchange Broadened NMR Spectra. Modified Version for Spin Systems Exhibiting Magnetic Equivalence or Symmetry," Program 165, Quantum Chemistry Program Exchange (1970).

44. B. W. Goodwin, M.Sc. Thesis, University of Manitoba (1969).

45. A. Allerhand and H. S. Gutowsky, J. Chem Phys., 41, 2115 (1964).

46. A. Allerhand, F. M. Chen and H. S. Gutowsky, J. Chem. Phys., 42 3040 (1964).

47. A. Allerhand and H. S. Gutowsky, J. Chem. Phys., 42, 4203 (1965).

48. H. S. Gutowsky and F. M. Chen, J. Phys Chem., 69, 3216 (1965).

49. A. Allerhand and H. S. Gutowsky, J. Am. Chem. Soc., 87, 4092 (1965).

50. H. S. Gutowsky, R. L. Vold and E. J. Wells, J. Chem. Phys., 43, 4107 (1965).

51. R. L. Vold and H. S. Gutowsky, J. Chem. Phys., 47, 2495 (1967).

52. T. D. Alger, H. S. Gutowsky and R. L. Vold, J. Chem. Phys., 47, 3130 (1967).

53. H. Y. Carr and E. M. Purcell, Phys. Rev., 94, 630 (1954).

54. K. H. Abramson, P. T. Inglefield, E. Krahauer and L. W. Reeves, Can. J. Chem., 44, 1685 (1966).

55. L. M. Jackman and F. A. Cotton eds., Dynamic Nuclear Magnetic Resonance Spectroscopy, Academic Press, New York (1975).

56. C. S. Johnson, Jr. and C. G. Moreland, J. Chem. Ed., 50, 477 (1973).

57. H. Schneider and G. P. Barker, Matrices and Linear Algebra, Holt - Rinehart - Winston (1968).

58. S. Brownstein and J. Bornais, Can. J. Chem., 46, 225 (1968).

59. N. A. Matwiyoff and W. E. Wageman, Inorganic Chemistry, 9, 1031 (1970).

60. J. R. Chipperfield and R. H. Prince, J. Chem. Soc., 3567 (1963).

61. L. H. Sommer and D. L. Bauman, J. Am. Chem. Soc., 91, 7045 (1969).

62. E. L. Muetterties and W. D. Phillips, J. Am. Chem. Soc., 81, 1084 (1959).

63. H. L. Mitchell and G. M. Whitesides, J. Am. Chem. Soc., 91, 2384 (1964).

64. M. Eisenhut, H. L. Mitchell, D. D. Traficante, R. J. Kaufman, J. M. Deutch and G. M. Whitesides, J. Am. Chem. Soc., 96, 5385 (1974).

65. R. S. Berry, J. Chem. Phys., 32, 933 (1960).

66. E. L. Muetterties, W. Mahler, K. J. Parker and R. Schmutzler, Inorganic Chemistry, 3, 1300 (1964).

67. H. Schmidbaur and H. Stuhler, Ang. Chem. Intl. Edn., 11, 144 (1972).

68. T. Furtsch, D. S. Dierdorf and A. H. Cowley, J. Am. Chem. Soc., 92, 5759 (1970).

69. H. Dreeskamp and K. Hildenbrand, Z. Naturforsch, 26b, 269 (1971).

70. C. G. Moreland, R. J. Beam, C. W. Wooten and S. M. Horner, Inorg. Nucl. Chem. Letters, 7, 243 (1971).

71. T. K. Davies and K. C. Moss, J. Chem. Soc. (A), 1054 (1970).

72. C. J. Hoffman, B. E. Holder and W. L. Jolly, J. Am. Chem. Soc., 62, 361 (1958).

73. E. L. Muetterties and W. D. Phillips, Adv. Nucl. Radiochem., 4, 248 (1962).

74. F. A. Cotton, J. W. George and J. S. Waugh, J. Chem. Phys., 28, 994 (1958).

75. W. M. Talles and W. D. Gwinn, J. Chem. Phys., 36, 1119 (1962).

76. K. Kimura and S. H. Bauer, J. Chem. Phys., 37, 3172 (1963).

77. E. L. Muetterties and W. D. Phillips, J. Am. Chem. Soc., 81, 1084 (1959).

78. E. L. Muetterties and W. D. Phillips, J. Chem. Phys., 46, 2861 (1967).

79. J. Bacon, R. J. Gillespie and J. W. Quail, Can. J. Chem., 41, 1016 (1963).

80. D. T. Sauer and J. M. Shreeve, J. Fluorine Chem., 1, 1 (1971-1972).

81. T. Abe and J. M. Shreeve, J. Fluorine Chem., 3, 17 (1973).

82. W. G. Klemperer, J. K. Krieger, M. D. McCreary, E. L. Muetterties, D. D. Traficante and G. M. Whitesides, J. Am. Chem. Soc., 97, 7023 (1975).

83. J. I. Musher and A. H. Cowley, Inorganic Chemistry, 14, 2302 (1975).

84. D. G. Ibbott, M.Sc. Thesis, University of Manitoba (1972).

85. R. K. Marat and A. F. Janzen, Unpublished results.

86. K. J. Wynne, Inorganic Chemistry, 10, 1868 (1971).

87. I. Solomon and N. Bloembergen, J. Chem. Phys., 25, 261 (1956).

88. A. N. Horner, J. Inorg. Nucl. Chem., 9, 98 (1959).

89. E. L. Muetterties and W. D. Phillips, J. Am. Chem. Soc., 79, 322 (1957).

90. J. C. Hindman and A. Svirmickas, In Noble Gas Compounds, Chicago (1963), Edited By H. H. Hyman.

91. R. J. Gillespie and G. J. Schrobilgen, Inorganic Chemistry, 15, 22 (1976).

92. R. G. Gordon and P. McGinnis, J. Chem. Phys., 49, 2455 (1968).

93. J. H. Wilkinson, The Algebraic Eigenvalue Problem, Clarendon Press, Oxford (1965).

94. C. M. Shepperd, M.Sc. Thesis, University of Manitoba (1970).

95. A. A. Frost and R. G. Pearson, Kinetics and Mechanism, John Wiley and Sons, Inc. (1953).

96. N. S. Ham and T. Mole, in Progress in NMR Spectroscopy, Ed. by: J. W. Emsley, J. Feeney and L. H. Sutcliffe, Pergamon Press (1969).

97. J. P. Maher and D. F. Evans, J. Chem. Soc., 5534 (1963).

98. R. K. Harris and K. M. Worvill, J. Mag. Res., 9, 383 (1973).

99. W. J. Moore, Physical Chemistry, Third edition, Prentice Hall, N. J. (1962).

100. W. E. Deming, Statistical Adjustment of Data, Wiley, N. Y. (1943).

101. W. F. Luder, P. B. Kraus, C. A. Kraus and R. M. Fuoss, J. Am. Chem. Soc., 58, 255 (1936).

102. J. Warf and M. Onyszchuk, Can. J. Chem., 50, 3450 (1972).

103. J. Warf and M. Onyszchuk, Can. J. Chem., 48, 2250 (1970).

104. H. C. Clark, K. R. Dixon and J. G. Nicolson, Inorganic Chemistry, 8, 450 (1970).

105. C. E. Burchill, Private Communication.

106. K. J. Laidler, Chemical Kinetics, McGraw Hill, Toronto (1965).

107. W. C. Gardiner, Jr., Rates and Mechanisms of Chemical Reactions, W. A. Benjamin, Inc., New York (1969).

108. R. Corriu and M. Leard, J. Chem. Soc. Chem. Comm., 1086 (1969).

109. R. Corriu and M. Henner-Leard, J. Organometal. Chem., 64, 351 (1974).

110. R. Corriu and M. Henner-Leard, J. Organometal. Chem., 65, C39 (1974).

111. R. J. P. Corriu and M. Henner, J. Organometal. Chem., 64, 1 (1974).

112. M. Gielen and H. Mokhtar-Jami, J. Organometal. Chem., 91, 633 (1975).

113. C. P. Poole, Jr. and H. A. Farrach, Relaxation in Magnetic Resonance, Academic Press, New York (1971).

114. A. Carrington and A. D. McLachlan, Introduction to Magnetic Resonance, Harper and Row, New York (1967).

115. R. E. Wasylishen, Private Communication.

116. T. C. Farrar and E. D. Becker, Pulse and Fourier Transform NMR, Academic Press, New York (1971).

117. P. Bird, J. F. Harrod and Khin Aye Than, J. Am. Chem. Soc., 96, 1222 (1974).

118. T. Axenrod and G. A. Webb, Nuclear Magnetic Resonance Spectroscopy of Nuclei Other than Protons, Wiley, New York (1974).

119. R. J. Hulett, Quart. Rev. 18, 227 (1964).

120. M. D. Alexander, Inorganic Chemistry, 5, 2081 (1971).

121. R. Koren B. Perlmutter-Hayman, J. Phys. Chem., 75, 2372 (1971).